

# Preliminary Design Studies for the Spectrometer Magnet for E161

## *RPC Technical Note #21*

Sebastian Kuhn  
Old Dominion University  
with L. Keller (SLAC) and P. Bosted (UMass)  
September - October 2001  
**FINAL VERSION 10/11/2001**

---

### **Abstract**

In this note, we present an alternative to the proposed spectrometer setup for SLAC experiment E161. The main feature of this setup is the use of a massive iron absorber inside the LASS dipole magnet, in the path of the decay muons, which will help to suppress non-muon backgrounds dramatically. At the same time, the increase in the integrated transverse magnetic field  $BdL$  in this configuration will counteract the increased multiple scattering of the muons, preserving roughly the resolution in transverse momentum  $p_T$  that would have actually resulted from the configuration described in the proposal.

A second variation is also considered where we put an additional short dipole magnet in front of the iron-filled LASS magnet. The additional increase in  $BdL$  increases the resolution further (at the expense of smaller acceptance), bringing it up to the resolution quoted in the proposal.

### **Introduction**

To maximize the signal/background ratio and count rate for E161, we have to achieve the following goals:

1. Good identification of muons
2. Good resolution in  $p_T$ , to separate muons from pion, kaon etc. decays from open charm decays
3. Large acceptance (up to  $p_T = 2$  GeV) to catch as many of the charm-decay muons as possible, and beginning at around 20 mrad to catch as many of the second muons from BH pairs as possible.
4. Excellent suppression of backgrounds, especially from hadrons and from small-angle  $e^+e^-$  pairs produced in the target as well as Compton-scattered photons.

**1)** The first criterion is best fulfilled by filling the spectrometer with an absorber up to as close to the target as possible, with as many hadronic Interaction lengths as compatible with the other criteria. The new spectrometer design outlined below consists of a straight flight path (of order 1 m) filled with alumina (and a dipole magnet also filled with alumina in the 2nd version) followed with 1.95 m length of solid iron. Very few particles other than muons will traverse this material to emerge in the first detector plane. An additional positive muon identification will be given by the 3rd hodoscope which is behind 50 cm of lead.

**2)** From [RPC Tech Note #6](#), we conclude that the resolution in  $p_T$  should be better than 0.12 GeV. For a background that falls like  $\exp(-9 \cdot p_T)$  (which seems to be typical for muons from kaon and pion decay) this results in an increase of the measured rate by a factor of 1.8, thereby decreasing the signal/background rate by about that factor (since the signal is more flat in  $p_T$ , it does not get enhanced as much by the resolution smearing). A detailed study of the different contributions to the resolution in  $p_T$  shows that at moderate values of  $p_T$  (0.5-0.7) the measurement error (standard deviation)  $\sigma(p_T)$  is roughly constant, but at higher  $p_T$  it begins to increase and ultimately becomes proportional to  $p_T / BdL$ . The size of  $\sigma(p_T)$  also depends on the total muon momentum (it gets somewhat worse with increasing  $p$ ), on the hodoscope

position resolution, and on the relative sign of the bend angle and the initial direction (inbending muons have **better** resolution than outbending ones!). While the  $p_T$  - proportional part of the resolution is inversely proportional to the integrated field  $BdL$ , it increases only like the square root of the total number of radiation lengths traversed. This makes it possible to replace a low- $Z$  material like alumina with iron (4.4 times shorter radiation length) if  $BdL$  is increased accordingly (ideally by a factor of 2).

**3)** This requirement involves a trade-off with high resolution (long magnetic field region) and hodoscope costs (number of channels for larger hodoscopes). The first variant of our new design discussed below maximizes the acceptance (nearly 100% up to  $p_T = 2.0$  GeV for  $p > 10$  GeV). at the expense of more hodoscope channels and somewhat marginal resolution. The second variant reduces the acceptance substantially (only 1/2 of the highest- $p_T$  muons are accepted within the "good resolution region", and only 22% of 6.5 GeV muons with  $p_T > 0.5$  GeV are accepted at all). However, due to the very low remaining background, this disadvantage can be somewhat offset by increasing the luminosity. In all cases there will be very good acceptance down to small angles (less than 20 mrad), resulting in a high likelihood that the second muon from a Bethe-Heitler pair will be detected in coincidence.

**4)** Hadrons and Compton-scattered photons will be completely contained by the massive iron wedge (12 interaction lengths and 110 radiation lengths). This is the main advantage of the new design presented here (previous studies have shown unacceptably high backgrounds from hadron "punch through", electron-positron pairs, and Compton scattering). Electrons and positrons from pair production in the target will be bent away by the full magnetic field into a Copper absorber with Tungsten lining, leading to a full containment of the resulting showers. The second version of our new design is preferable for this purpose, as well.

An additional consideration which has not been emphasized in the proposal is the capability to reconstruct  $J/\psi$  decays. While the theoretical interpretation may be more difficult, this channel is potentially much cleaner experimentally (since little background from other hadronic decay is present). To get a reasonable signal/noise, we estimate that the resolution in reconstructed mass should be better than 10% at the  $J/\psi$  peak (3.1 GeV). This can be achieved with the second version for all muon momenta, but not with the first version of our new design.

## Design Considerations

The basic idea of our new design is to increase both the absorption length and the integrated magnetic field  $BdL$  by guiding the field generated by LASS through a 1.95 m long, 1.01 m high iron "wedge" that fills out the height of the magnet gap and concentrates the field in the "acceptance volume" for muons. The wedge will be centered horizontally in LASS, but the front end will extend about 45 cm before the top and bottom return yokes, while the rear end will extend 40 cm beyond those yokes. The wedge flares out in the horizontal plane roughly along  $\pm 200$  mrad lines. Specifically, the front face of the wedge will be 80 cm wide ( $\pm 40$  cm from the symmetry plane) while the back face will be 160 cm wide ( $\pm 80$  cm). This is well matched with the planned acceptance and size of the hodoscope planes in our design. The wedge will have a 2cm thick slab cut out in its midplane, where the iron is replaced by copper. The copper has a central "hole" of 1.6 cm ( $\pm 0.8$ cm) accommodating the beam pipe, to allow the photon beam to pass through undisturbed. The absence of magnetic material in this midplane gap guarantees that the full magnetic field of up to 2T will be present across the beam profile, to sweep out any charged particles (especially electrons and positrons from pair production). At a field of about 1.9 T, it takes at most 1.2 m distance to deflect a 48 GeV singly-charged particle by at least 0.8 cm sideways. To make sure that any showers generated by particles swept out of the beam in this manner are fully contained, we can replace the first few cm width of copper adjoining the beam pipe with tungsten.

One welcome advantage of filling the LASS gap with iron is that we will need significantly less current to achieve high fields than for an air (or alumina) gap magnet. LASS as presently configured has 648 windings

of Cu coil and can be run in excess of 7000 Amps (split between two parallel coil circuits), leading to a total excitation of 2268 kAturns. Our preliminary studies show that a useful field of up to 2 T can already be reached with 2500 A (810 kAturns), corresponding to a reduction of the needed electrical power to about 625 kW (an important benefit in light of the expected high costs of electricity during E161 running).

In the first version of our design, the wedge will begin about 1.20 m after the polarized target center. This space is filled with alumina to suppress pion and kaon decay muons. The front mirror plate (needed to protect the polarized target solenoid against strong transverse fields) will begin 80 cm behind the target center. We assume that the first hodoscope "superplane" will be situated 17 cm behind the rear mirror plate (3.9 m from the target center) and will cover an area of 130cm x 120 cm (horizontal x vertical). The second "superplane" will be 90 cm behind the first one, covering 200 cm x 150 cm, followed by a 50 cm lead absorber and a final plane covering 240 cm x 160 cm. This last plane does not require high resolution and could be made of the UVa/Basel neutron bars (10x10x160 cm each, with phototubes on both ends). 24 of these bars placed vertically could cover the necessary area and give us an additional point in time and space for tracks which are most likely muons.

The second version is similar, except that the distance to the polarized target is increased to 2.15 m and the additional space is used to install a second magnet (29D36) in front of LASS. This magnet (presently in the SLAC magnet lab) has an integrated BdL of about 22 kGm and is small enough that its coils **might** fit inside the LASS coils (needs to be checked!). It has a physical (effective) length of about 90 cm (110 cm) and would have to be fitted with a mirror plate at its upstream end, once again to protect the polarized target against strong transverse fields. Both due to the additional target-detector distance and due to the rather small gap height of 25.4 cm of this magnet, the acceptance of this arrangement is substantially smaller (especially in the y-direction). The horizontal gap size is 74 cm, which is nicely matched to the wedge entrance width. The reason to add this magnet is that due to the higher total BdL the resolution will be better. However, the larger bend angles achieved require larger hodoscopes in the horizontal direction than the first version, which is mostly offset by their smaller size in y (because of the limited aperture in that direction). We foresee a first hodoscope superplane (4.8 m from the target center) of size 180cm x 80 cm (horizontal times vertical) followed by a second one (90 cm downstream of the first) of size 250 cm x 100 cm. The muon identifier should cover 300 cm x 120 cm which once again can be accomplished with (in this case) 30 vertical neutron bars. One other drawback of the second version is that muons below 6.5 GeV are not accepted very well at all, since they lose too much energy and get bent by more than 420 mrad.

Ultimately, a full 3-dimensional simulation (supported by magnetic measurements) will be needed to optimize either one of these designs. As an initial, preliminary "proof of principle", we ran several simulations in an approximate 2-dimensional model, using the code "Mermaid".

## **Simulation with "Mermaid"**

The code "Mermaid" by SIM Limited (Novosibirsk, 1994) is a 2D field simulation code (with a built-in 3D extension), based on the familiar "Poisson" code but with an improved graphical interface. It runs on DOS, Windows and Windows NT machines. Simulations can be made for magnets (and coils) which extend "infinitely" in one direction, with arbitrary cross section which has to be laid out on a triangular "logical mesh".

Clearly, this method is not directly applicable to LASS with a wedge-shaped iron filling, since the dimensions perpendicular to the longitudinal cross section (midplane) are not infinite (not even constant). In addition, the flux is returned "out of plane" in the real magnet, which has to be simulated by an artificial "return leg" in the 2D simulation. In our simulation, we kept the longitudinal cross section of the wedge unchanged, but increased the horizontal dimensions of the return path relative to its true dimensions (1.1 m all around) proportional to the cross sectional area through which the field lines have to go, relative to the average horizontal cross sectional area of the wedge ( $1.95 \times 0.6 \text{ m}^2$ ).

Flux from: -44.2550                      To: 3497.63                      Step: 70.8376  
Xmin= 0.000000                      Ymin= 0.000000  
Xmax= 500.000                      Ymax= 368.000

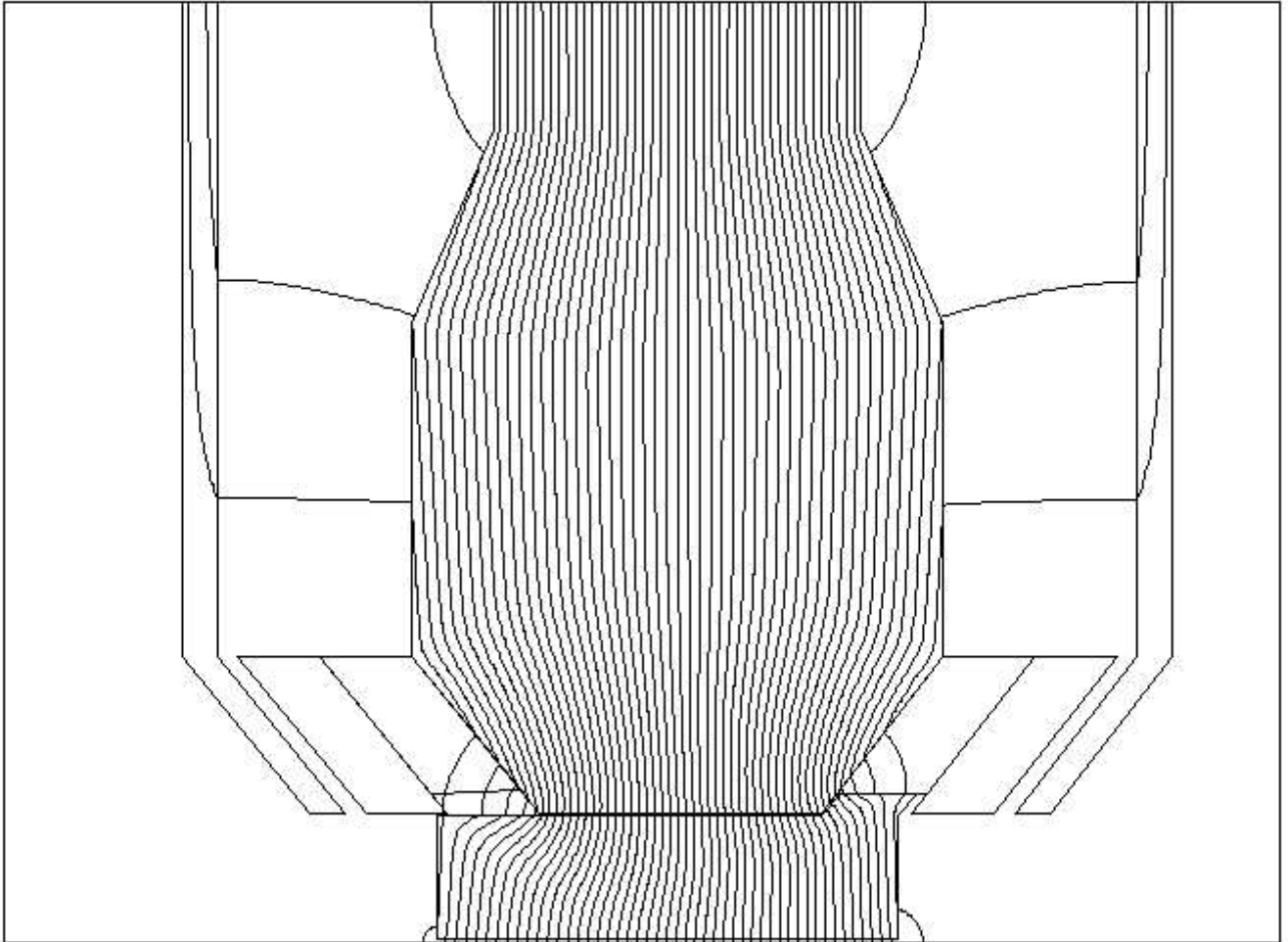


Figure 1 shows the layout of the 2-dimensional simulation used, together with the field lines generated by "Mermaid". The bottom rectangle is the wedge, followed by the return leg of variable width. The wedge has a "hump" in the back which fits into a gap left by the innermost LASS coils (the slanted parallelograms represent the coils across the front and back faces of the top yoke of LASS). This "hump" improves the field homogeneity and strength at the exit face of the wedge. (In the final design, we will likely put such a "hump" in the front, as well). The "fingers" simulate the mirror plates. While the spatial arrangement of field lines in the top half of this figure cannot be translated literally, the lines outside the iron return legs show that the iron is close to saturation, leading to non-zero magnetic fields in the vicinity of LASS which is effectively shielded by the mirror plates.

Distribution of			Bt										
Xmin=	169.567		Ymin=	0.000000									
Xmax=	430.433		Ymax=	184.000									
16*2	16*2	16*2	16*2	16*3	16*3	16*3	16*3	16*3	16*3	16*3	0.92	0.91	0.89
16*3	16*3	16*3	16*3	16*4	16*4	16*4	16*4	16*4	16*4	16*3	0.93	0.91	0.90
16*3	16*3	16*4	16*4	16*4	16*4	16*4	16*4	16*4	16*4	16*4	0.94	0.92	0.90
16*4	16*4	16*4	16*5	16*5	16*5	16*5	16*4	16*4	16*4	16*4	0.95	0.93	0.90
16*4	16*4	16*5	16*6	16*6	16*6	16*6	16*5	16*5	16*5	16*5	0.95	0.95	0.91
16*3	16*4	16*6	16*8	16*8	16*8	16*7	16*6	16*5	16*5	16*5	0.97	0.96	0.92
16*2	16*3	16*9	17*1	17*1	17*1	16*9	16*7	16*5	16*4	16*4	0.98	0.99	0.93
15*9	16*6	17*4	17*7	17*6	17*5	17*3	16*9	16*5	16*3	16*3	1.00	1.02	0.95
15*4	16*6	18*1	18*6	18*2	18*1	17*9	17*4	16*6	15*9	15*9	1.00	1.08	1.00
16*6	17*6	18*1	18*6	18*8	18*8	18*6	18*1	17*2	16*0	16*0	0x91	0x82	0x82
17*7	18*5	19*0	19*5	19*7	19*7	19*5	19*0	18*2	17*4	17*4	0x47	0x42	0x53
18*5	19*2	19*9	20*4	20*6	20*6	20*4	20*0	19*2	1x50	1x50	0x58	0x11	0x37
2x67	20*1	20*6	21*2	21*4	21*5	21*4	21*0	20*2	2x03	2x03	0x86	0x23	0x19
3x38	21*0	21*5	22*1	22*2	22*3	22*3	22*0	21*2	2x48	2x48	1x07	0x49	3*74
4x07	22*0	22*4	22*8	22*8	22*9	23*1	23*2	22*5	3x05	3x05	1x18	0x78	3*47
4x43	23*2	23*4	23*4	23*3	23*4	23*7	24*5	7x65	7x65	7x65	1x07	1.05	0.06
4.54	0.67	24*7	23*8	23*4	23*5	23*9	25*6	17*5	3x00	3x00	1x07	4*89	0.08
12*7	18*2	23*9	23*1	22*8	22*6	22*4	20*4	19*2	0x63	0x63	1x07	4*89	0.08
14*8	16*4	21*4	22*1	22*0	21*7	21*1	20*4	20*0	0.65	0.84	0.63	0.10	
16*3	15*8	19*4	20*9	21*1	21*0	20*7	20*4	20*2	0.70	0.69	0.40	0.10	
17*1	17*1	17*9	19*7	20*3	20*4	20*4	20*3	20*2	0.75	0.60	0.31	0.10	
17*7	17*6	17*9	18*8	19*5	19*9	20*0	20*0	20*1	0.84	0.56	0.26	0.09	
17*9	17*8	18*0	18*4	19*0	19*4	19*6	19*6	19*8	1.06	0.55	0.24	0.08	
									1.41	0.55	0.23	0.08	

Figure 2 shows a coarse sample of total magnetic field values calculated by "Mermaid" near the wedge. All values are in kG (multiply with 0.1 to get Tesla). One can see that the iron at the interface between wedge and return yoke is highly saturated (24 - 26 kG), while most other regions are only moderately saturated. The field fills the useful volume of the wedge quite uniformly (from 18 to 20 kG in the areas that can be traversed by muons).

Graph: Bx and By Min: -20.0000 Max: 5.00000  
Line: ( 100.000 , 0.00000 ) -> ( 400.000 , 0.00000 )  
Integrals: 0.942599 and -3450.84

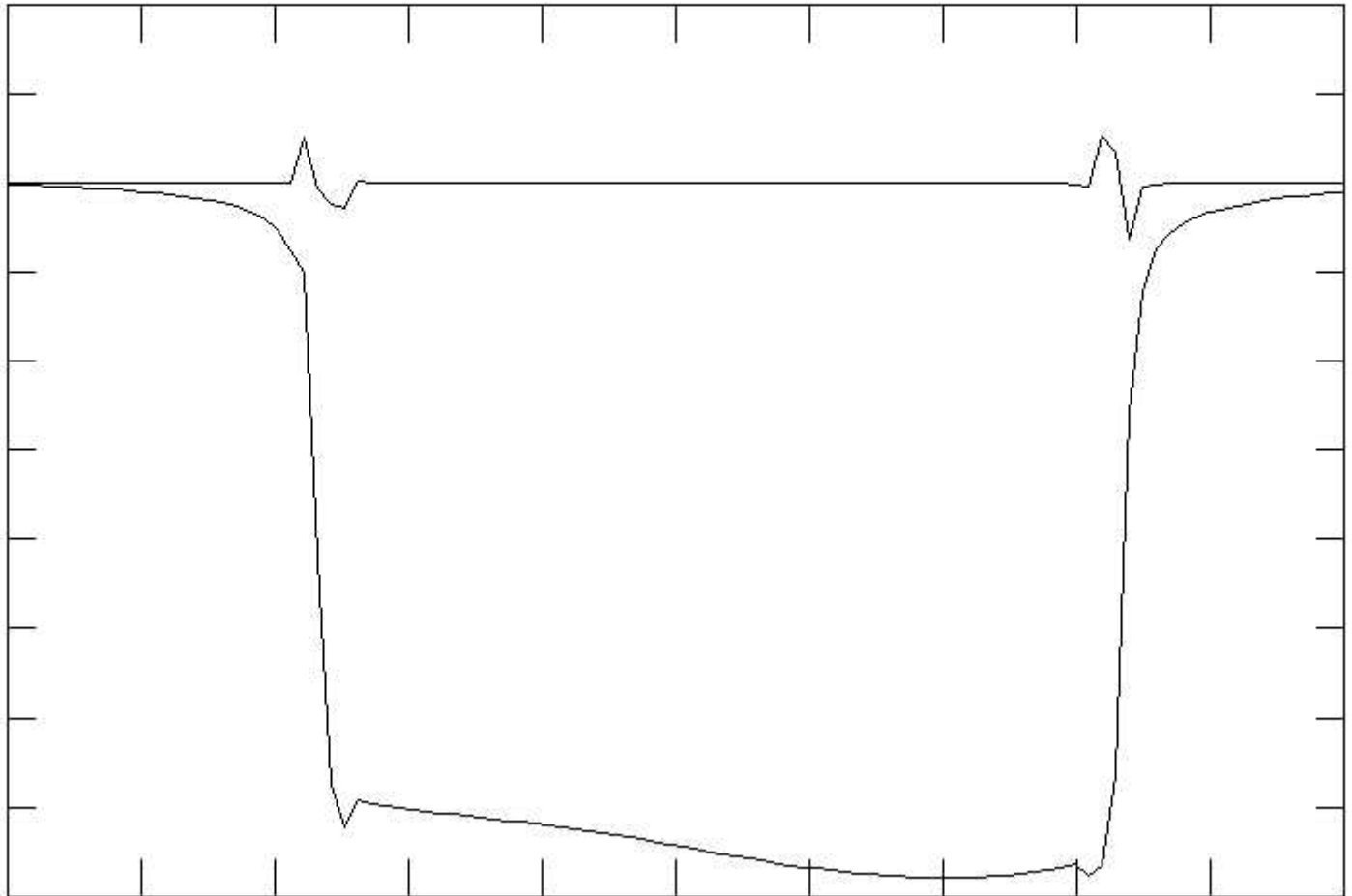


Figure 3 shows the magnetic field profile (both the vertical - bottom - and the horizontal - top - component) along a line beginning 70 cm before the wedge and ending 50 cm after its end, in the air/copper gap at the center of the wedge. The vertical scale ranges from +0.5 T to - 2 T. The integrated BdL along this line is 3.4 Tm according to this calculation. which corresponds to an average field of 1.9 T over the physical length of 1.8 m. A final simulation with a 1.95 m long wedge and 2500 A excitation yielded an integrated BdL of 3.65 Tm (average field of 1.87 T).

Due to the mirror plates (which turn out to be absolutely crucial), the residual field in the polarized target region is less than 5 Gauss, with a negligible gradient of a few G/cm (note that these fields add perpendicularly to the main target field, changing it by an infinitesimal amount). The field right next to the rear mirror plate, 15 cm behind it, where the phototubes of the first hodoscope plane will be situated, is of order 20-40 G, which can be easily shielded with mu-metal shields around the phototubes.

An additional MERMAID study was conducted to look at the effect of the massive iron plates of LASS close to the target solenoid (the mirror plates are only 80 cm downstream of the target center). If we assume a solenoid of 90 cm length and average winding radius of 10 cm, we find we need about 5 MAWdg to get a 7 T field on axis. The effect of LASS on this field is minimal; the only noticeable effect was an introduced

gradient of 1.13 G/cm at the center of the solenoid. This could be compensated with the separately adjustable trim coils already foreseen in the present design of the target solenoid (using the "NMR" magnet design).

One other concern arising from the vicinity of LASS to the polarized target is the force exerted on the latter. In addition to distorting the central field of the solenoid slightly, we also find that the solenoid is attracted towards the upstream mirror plate with a force of about 80 kg. In addition, any non-zero perpendicular field (even a few Gauss) from LASS in the region of the solenoid windings would create a torque that will try to align the solenoid along the vertical. This torque could be of order a few kg-m. This additional force and torque on the solenoid must be taken into consideration in the design of its suspension.

We also ran a simulation of the second design version, with the magnet 29D36 in front of LASS. Our simulation indicates that we need 600 kA-turns to achieve a BdL of 2 Tm, **which needs to be checked** against the actual capabilities of this magnet. In that case, the two fields add up linearly (no interference between the wedge and this dipole) to give a total BdL of 5.67 Tm. The two magnets **will** repulse each other, of course; a **very** crude estimate with MERMAID yielded a few tons of force (which is fully contained by the necessary "earthquaking" anyway).

To minimize the loss of acceptance, we would like to put the polarized target as close to this magnet as possible. Assuming some reasonably sized mirror plate, we hope that we can "get away" with only 80 cm between the target center and that mirror plate. This would not increase the force on the polarized target solenoid too much (about 190 kg), but it would increase the unwanted gradient of B to 11 G/cm. If this cannot be compensated by the trim coils, we will need to move the target further upstream until a reasonable compromise is reached.

## Field Measurements with LASS

On October 2, 2001, we tested the performance of the LASS magnet in its present configuration. We ran currents up to 2700 A (corresponding to 874 kA-turns) and measured the voltage drop, return water temperature and magnetic fields. The equivalent resistance of LASS together with the current cables from the power supply was very close to 0.1 Ohm. This means that we used as much as 730 kW of power (LASS is designed for nearly 5 MW of power) which warmed the return water from 86 F to about 110 F. Extrapolating to the expected 2500A current for E161 running (with wedge), we will need about 625 kW - both existing supplies and cables and water lines are ample for this purpose.

We took several measurements of the magnetic field generated by LASS, both as a function of current I and as a function of position at fixed  $I=2500\text{A}$ . Most of the data we took are summarized in [this postscript file](#). This file contains both our data (symbols) and the "prediction" (lines) using MERMAID (see below).

The first graph shows the magnetic field (in Tesla) at 3 locations, measured vs. current I. The solid line and the "x"es refer to the point in the center of the magnet ( $x=y=z=0$ ) halfway between the yokes; the dashed line and diamonds refer to the center ( $x=z=0$ ,  $y=-50.5\text{ cm}$ ) of the surface of the bottom yoke (at the bottom of the gap), and the stars and dotted line refer to a point very close to the edge of the bottom yoke ( $y=-50.5\text{ cm}$ ,  $z=55\text{ cm}$ ), centered between the coils ( $x=0$ ). The agreement between MERMAID and our measurements is very good except for the last case, which is due to the extreme sensitivity of the field on the exact probe position and local magnetic properties of the yoke iron.

The second graph shows results for the z-dependence of the magnetic field at a fixed current of 2500 A. z is measured from the center of the return yokes. The solid line and "x"es refer to the symmetry axis ( $x = y = 0$ ), while the dashed line and diamonds refer to a line centered in x ( $x=0$ ) but at the bottom of the gap (yoke surface,  $y=-50.5\text{ cm}$ ). The stars refer to a line along the bottom right corner of the gap (touching the bottom yoke and the coil surface;  $x = 90\text{ cm}$ ,  $y = -50.5\text{ cm}$ ). This line cannot be simulated properly in a 2D code, so

there are no MERMAID results to compare to. However, a second simulation of the cross sectional view of LASS as well as our data showed that the field tends to be very homogeneous in x from one coil to the other. The agreement for the field along the center line is not so good, but this may be partially due to a measurement uncertainty (the probe had to be held up in the air and approximately centered in x and y).

The MERMAID model used in this study was once again a longitudinal cross section, as described above, with fanning "return legs" to simulate the actual cross section seen by field lines. We tested both tables for  $\mu$  vs. B that correspond to "semi-realistic steel", numbered 4 and 6 in the MERMAID (and POISSON) code. While both  $\mu$  tables give acceptable agreement with our actual measurements, we also compared calculated fields and field integrals for much higher currents with those quoted in the literature on LASS (SLAC-298). We concluded that only table 6 can describe the behavior of LASS reasonably over its full range of current excitation. This gives us further confidence that the results of our simulations with the wedge are not totally unrealistic; however, a direct measurement of the  $\mu(B)$  curve of "typical" LASS steel (using a sample from the actual magnet) would increase our confidence that this curve is modelled correctly. All simulations described in this Technical Note were done using  $\mu$ -table 6.

During our test measurements, we noticed that the dimensions of LASS are quite different from the simplified model we had been working with so far. In particular, the coils use up less volume and the return legs are more massive than shown on a simple drawing we used up to then. On the other hand, the coils are not only smaller, but also not quite symmetric (front and back). Finally, it appears that in its present configuration in ESA, LASS is missing one of its return yoke plates at the top, leading to less iron on top than on the bottom. While our model indicates that this may not be a problem, it would be prudent to install this missing plate (which has been stored on the ESA floor, together with the mirror plates). All simulations quoted in this Technical Note use the actual configuration of LASS as we found it, including the missing top plate.

## Hodoscopes and Resolution

We used a modified version of the simple tracking program "spect.f" to simulate both versions of our new design. This code includes a fairly realistic simulation of energy loss, multiple scattering (calibrated against the full Moliere theory) and track reconstruction with finite hodoscope resolution and target point uncertainty, and calculates the resolution in  $p_T$  and acceptance. We found that to achieve the best possible resolution, the track reconstruction must use the information from both the y-position and the slope (angle)  $dy/dz$  at the exit of the spectrometer, to correct at least partially for multiple scattering. Otherwise, the bad resolution in  $dy/dz(0)$  will inflate the resolution in  $p_T$  significantly. We found an empirical formula for the initial scattering angle in the y-plane:  $dy/dz(0) = 1.5 y(1)/z(1) - 0.5 dy/dz(1)$  (at the position of the first hodoscope). To utilize this information, one cannot make the resolution in y too coarse for the first 2 hodoscope planes.

In an initial step, we used a uniform hodoscope position resolution of 0.25 cm, which would result if we would cover the full hodoscope area with 2 planes each in x and y of 1/2" wide fingers, with a 1/4" offset between the planes. (These 4 planes together are referred to as "superplane" in this document). The results of this simulation for the first version (LASS only) can be found in [LassOnly.ps](#). The first 3 graphs show the resolution  $\sigma(p_T)$  vs.  $p_T$  for initial muon momenta of 6 GeV, 10 GeV and 15 GeV, respectively. The resolution is 0.12 GeV (0.14 GeV, 0.16 GeV) for low  $p_T$  and increases slowly with  $p_T$ , as advertised. The acceptance for muons above  $p_T = 0.5$  GeV is 54% (98%, 100%) for the 3 initial momenta. The file [LassOnly.ps](#) also contains the acceptance vs.  $p_T$  (in the next 3 graphs; the histogram shows the thrown events, the solid line shows the accepted events and the dashed line shows the accepted events smeared with the resolution). Sample tracks for the 3 initial momenta and "typical" hits on the hodoscope planes are also shown.

For the second version, the average  $p_T$  resolution is 0.09 GeV (0.116 GeV, 0.129 GeV), a clear improvement. On the other hand, the acceptances are only 18% (73%, 96%). The position resolution assumed here would result in an unrealistic large number of channels of about 1900. We have tried to reduce the number of channels while maintaining the good resolution of version 2 as much as possible, and making optimal use of existing fingers from E155x. A possible scenario would look like follows:

In the first hodoscope "superplane", we would cover  $\pm 61$  cm width in  $x$  for each quadrant with vertical ( $x$ -measuring) fingers of 1/2" width, overlapping in two adjacent planes as before. The same would be done for the first  $\pm 71$  cm of the second "superplane". This requires a total of 832 fingers, with 310 suitable ones already in hand (although most have to be lengthened to 40 or 50 cm for the first/second superplane). The next 16 cm in the first superplane can be covered with existing 1.5 cm fingers, and the remaining 15 cm (for a total of 92 cm in each quadrant) with existing 1" fingers. In the 2nd superplane, we would add 8 cm with existing 2 cm fingers, 15 more cm with 48 new 1" fingers and the remaining 30 cm with existing 3 cm fingers for a total of 124 cm in each quadrant. In each case, the fingers would be arranged in two overlapping planes. The horizontal ( $y$ -measuring) fingers would be all new 1" wide (288 needed for 2 overlapping planes in each quadrant and both superplanes). In total, 858 new instrumented fingers would be needed (522 1/2" width and 336 1" width), and 558 existing fingers could be reused after bringing them to the proper length, for a total of 1416 channels (plus 30 more for the "muon hodoscope" made of UVa n detector bars). This is clearly an increase in the total number of channels beyond the original design, but is required to maintain the good resolution of version 2 at least for inbending muons.

A full simulation for this scenario has been done as well, with results in [LassReal.ps](#). The plots show results for  $p_0 = 6.5$  GeV, 10 GeV and 15 GeV. In addition, the first 6 plots show both positive and negative values for  $p_T$ , where the negative values refer to inbending muons and the positive values to outbending ones. It is obvious that inbending muons will have much better resolution in  $p_T$ , both because of a compensation of errors in  $p_0$  and  $dx/dz(0)$  and because we put all high-resolution fingers (1/2") in that region. The numerical values for the resolution below  $p_T = 1$  GeV are 0.092, 0.12, 0.14 GeV for 6.5 GeV, 10 GeV and 15 GeV muons, respectively. For 10 GeV and 15 GeV, there is still some acceptance (and reasonable resolution) for outbending muons up to  $p_T = 1$  GeV, as well, while outbending muons below 6.5 GeV are not accepted at all. Since only inbending muons would be used for  $J/\psi$  reconstruction, a mass resolution of better than 9% would be maintained according to this simulation.

## Results and Conclusions

Our preliminary simulation shows that we can achieve good momentum resolution of the E161 spectrometer while increasing the shielding against non-muonic particles drastically by filling the "acceptance volume" of LASS with massive iron and placing an additional short dipole in front of it. (We will probably fill the remainder of the LASS gap with lead.) Extensive simulations of the magnetic fields in a 2D model and of the resulting spectrometer performance were done and confirmed the basic parameters of this design. From this preliminary study, the new design of the E161 spectrometer seems viable; however, a 45% increase in the total number of required hodoscope channels seems unavoidable.

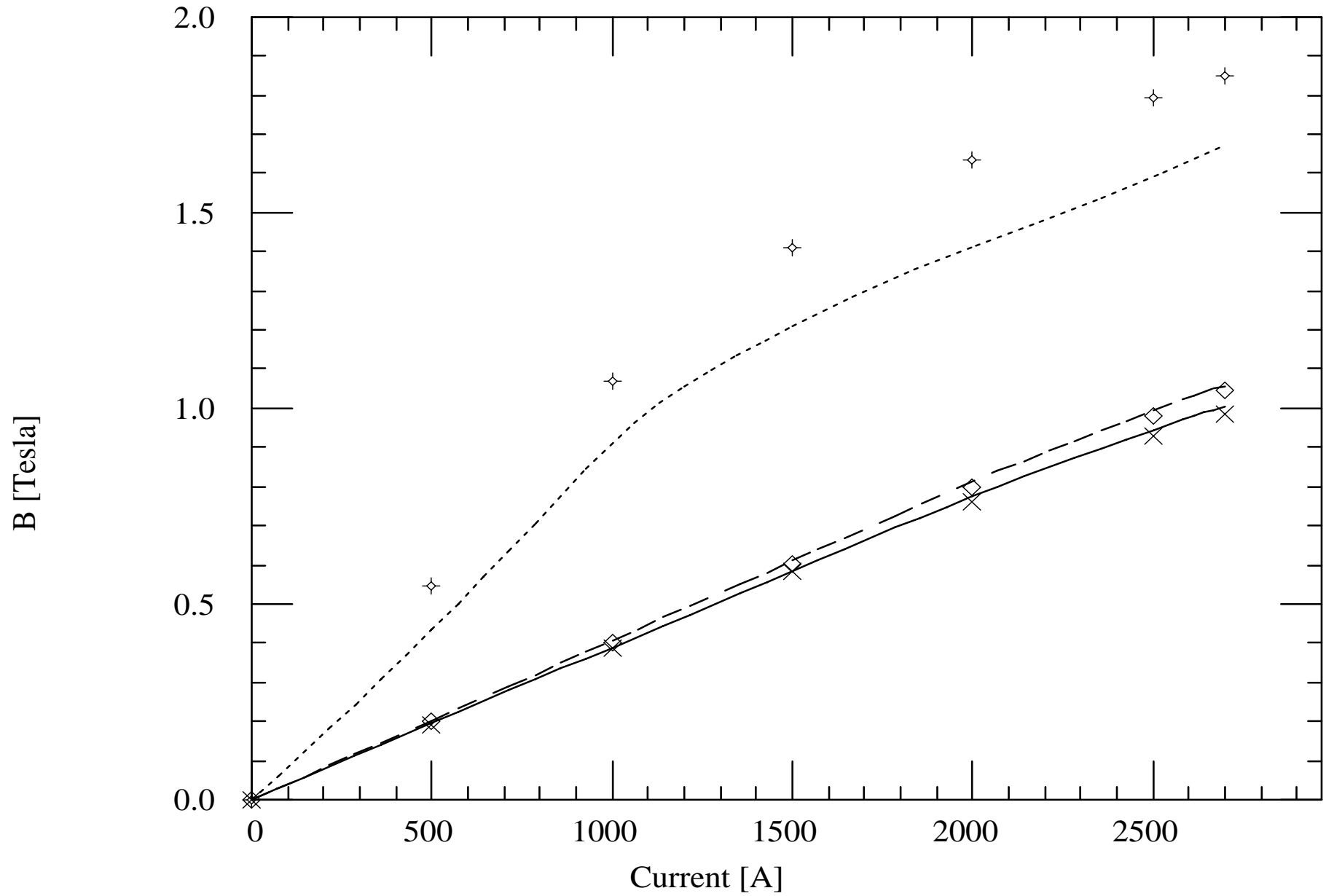
The following needs to be done to verify this design

1. A more realistic, 3-dimensional model of the magnetic field produced by the magnet-wedge arrangement, including magnetic forces, fringe fields etc. This includes magnetic shielding requirements for the phototubes of the first hodoscope plane after LASS and compensation coils for the polarized target. The exact dimensions of the wedge (length between 1.6 and 2.0 m) versus achievable integral  $BdL$  for both versions should be studied to help decide on the best trade-off between resolution, acceptance and hodoscope coverage. See also point 4 below for additional ideas for "sculpting" the wedge to achieve optimal transport of field lines.

2. A more realistic simulation of actual muon tracks through the whole spectrometer, including multiple scattering and energy loss, detector resolution and track reconstruction, and separation of muons coming from charm decays, J/psi decays, Bethe-Heitler muon pairs, and other hadronic decays.
3. A more detailed study of signal/background ratios in this scenario, with reliable estimates how well we can extract the charm-decay signal from all other sources of muons. This includes verification that both electromagnetic showers from pair-produced electrons and positrons are well contained, and hadronic punch through is minimal (initial studies by P. Bosted indicate that this is indeed the case, with the possible exception of signals from low-energy neutrons and pions "leaking" out).
4. A more detailed engineering design, including possible sources of the iron needed for the wedge (one could consider building the wedge out of thin plates of varying lengths and width 0.49 m that would be stacked on edge, side by side, with thin insulators in between to reduce eddy currents). Additional studies should be done to optimize the overall wedge dimensions (e.g., it need not flare out quite as much in the back, but for compatibility with E160 it might need to have a larger front face. Also, the field homogeneity and strength might be improved by increasing the interface area between the LASS return yokes and the wedge, to reduce saturation in that area. This could be done by adding "flares" that increase the width of the wedge at its top and its bottom, and another "hump" in the front to take advantage of the exposed yoke side).

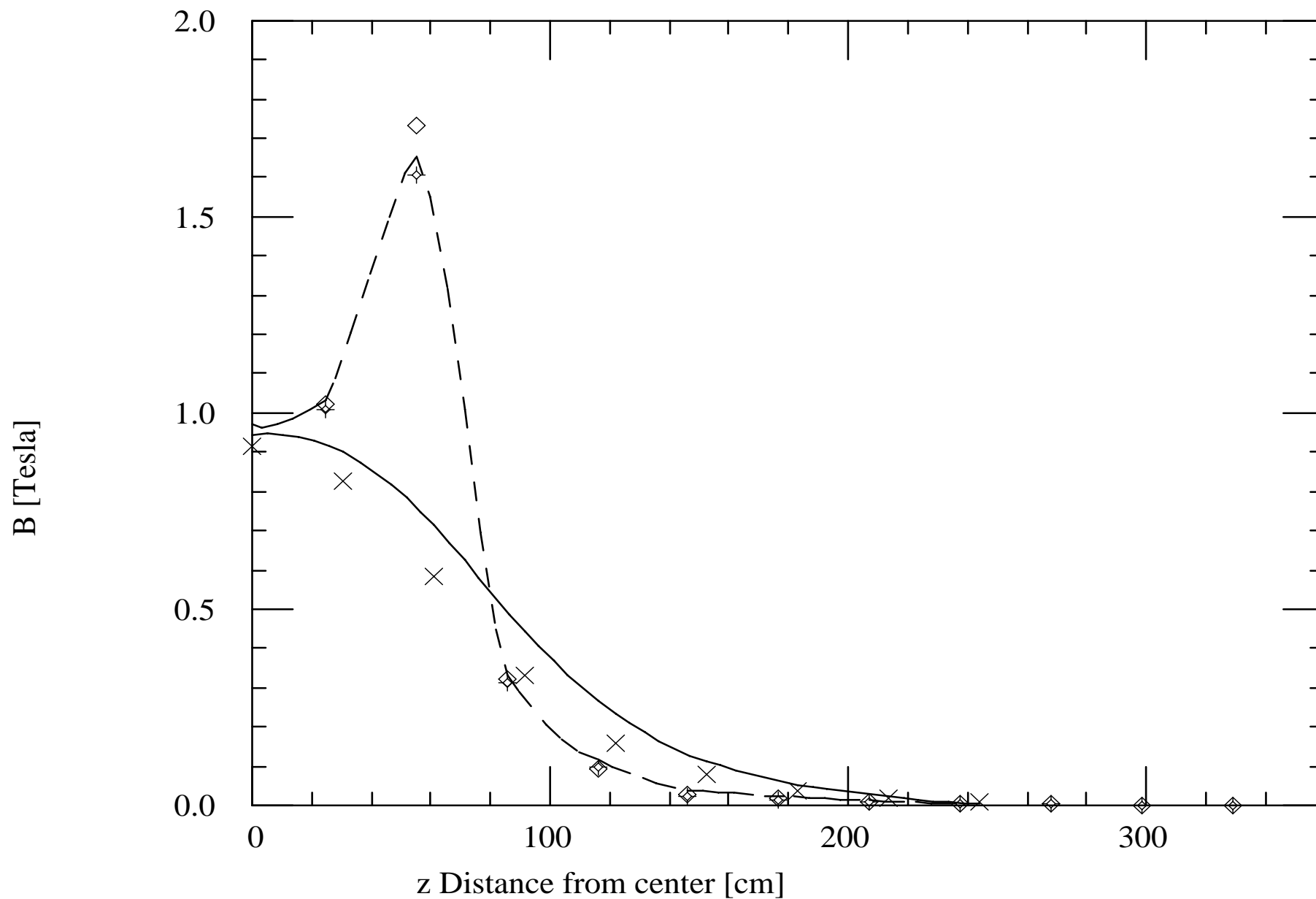
# Lass field center, bottom ctr, yoke edge

LASS test fig. 1

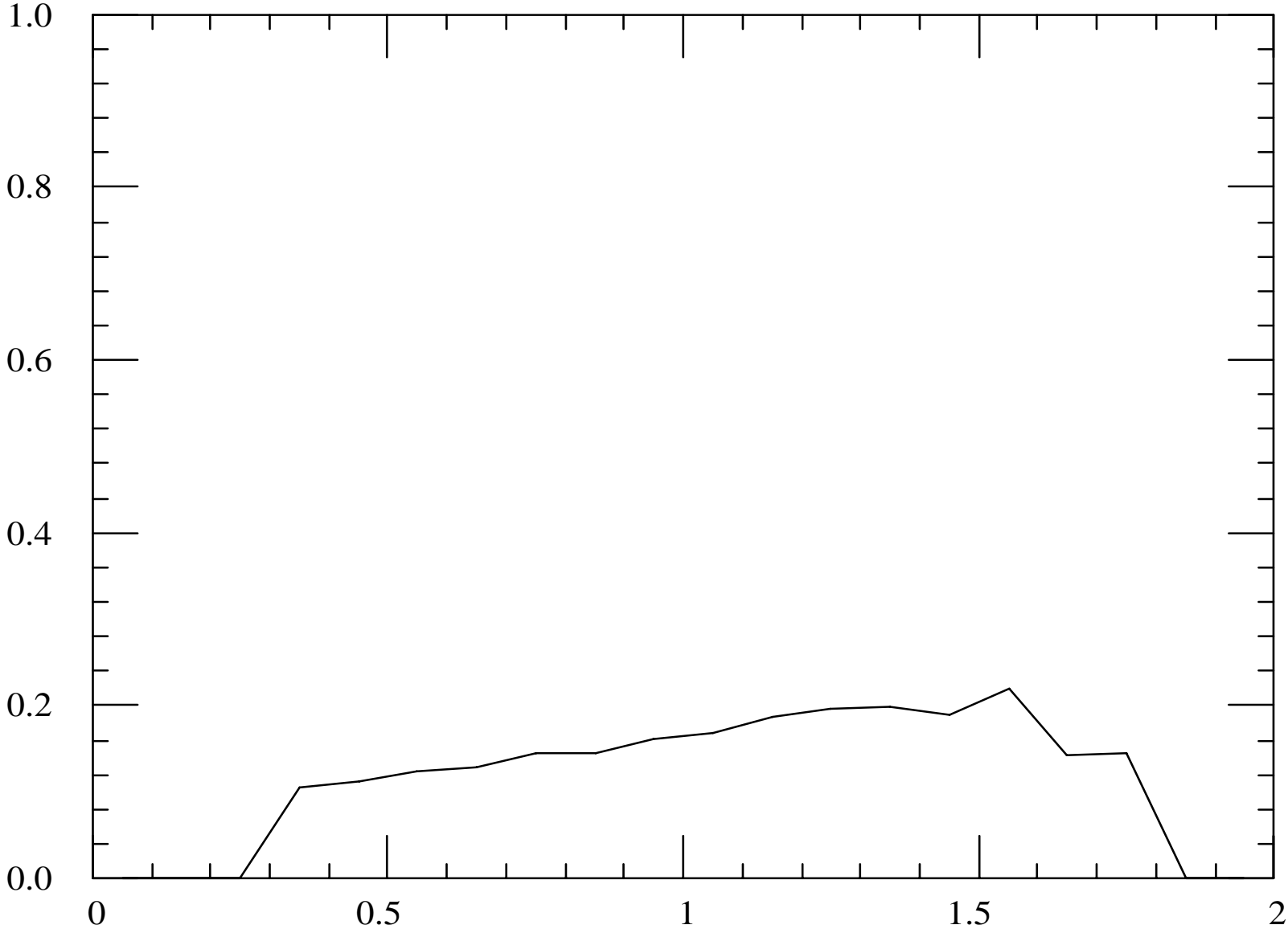


# Lass field center, bottom ctr, corner

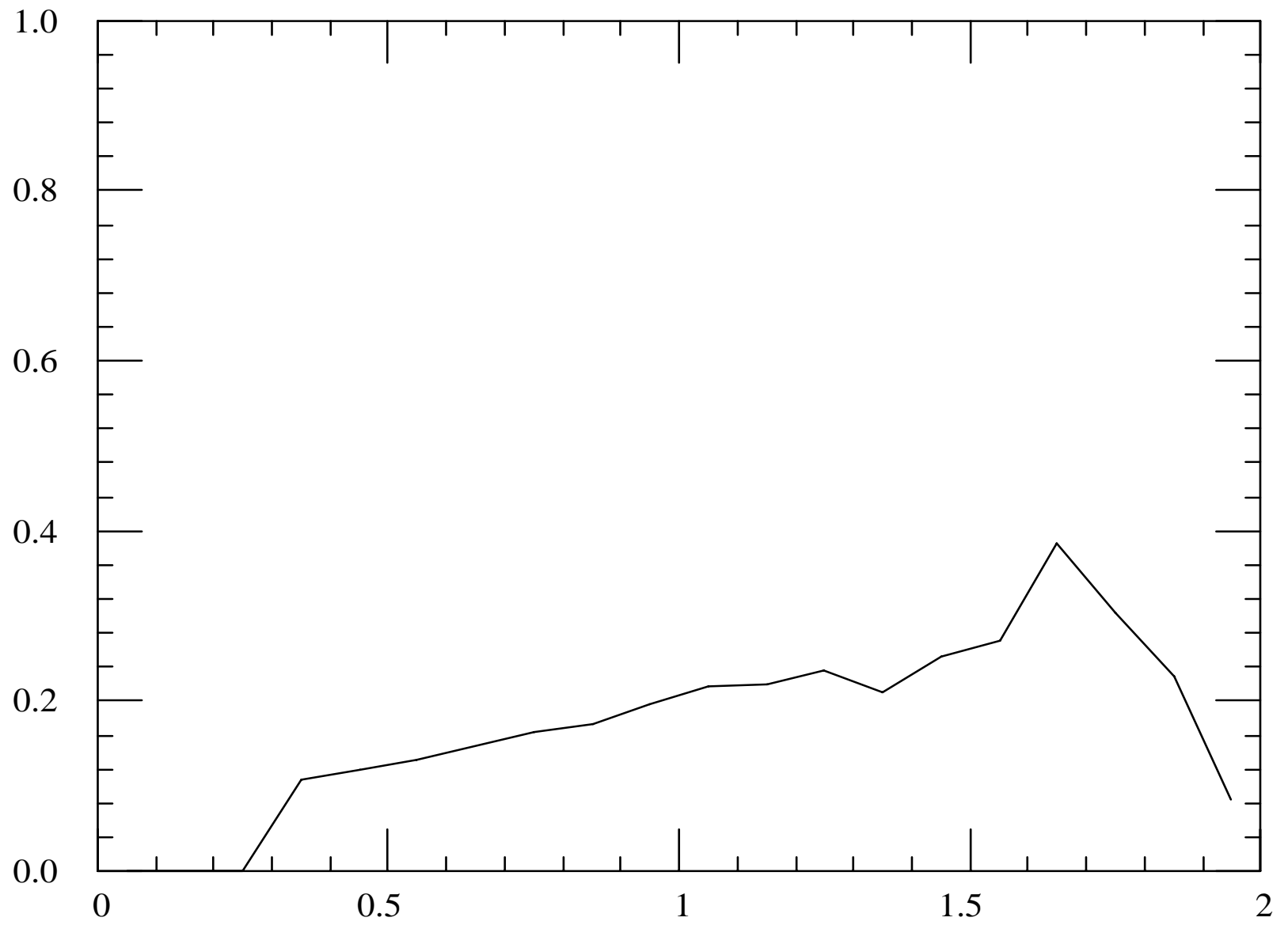
LASS test fig. 2



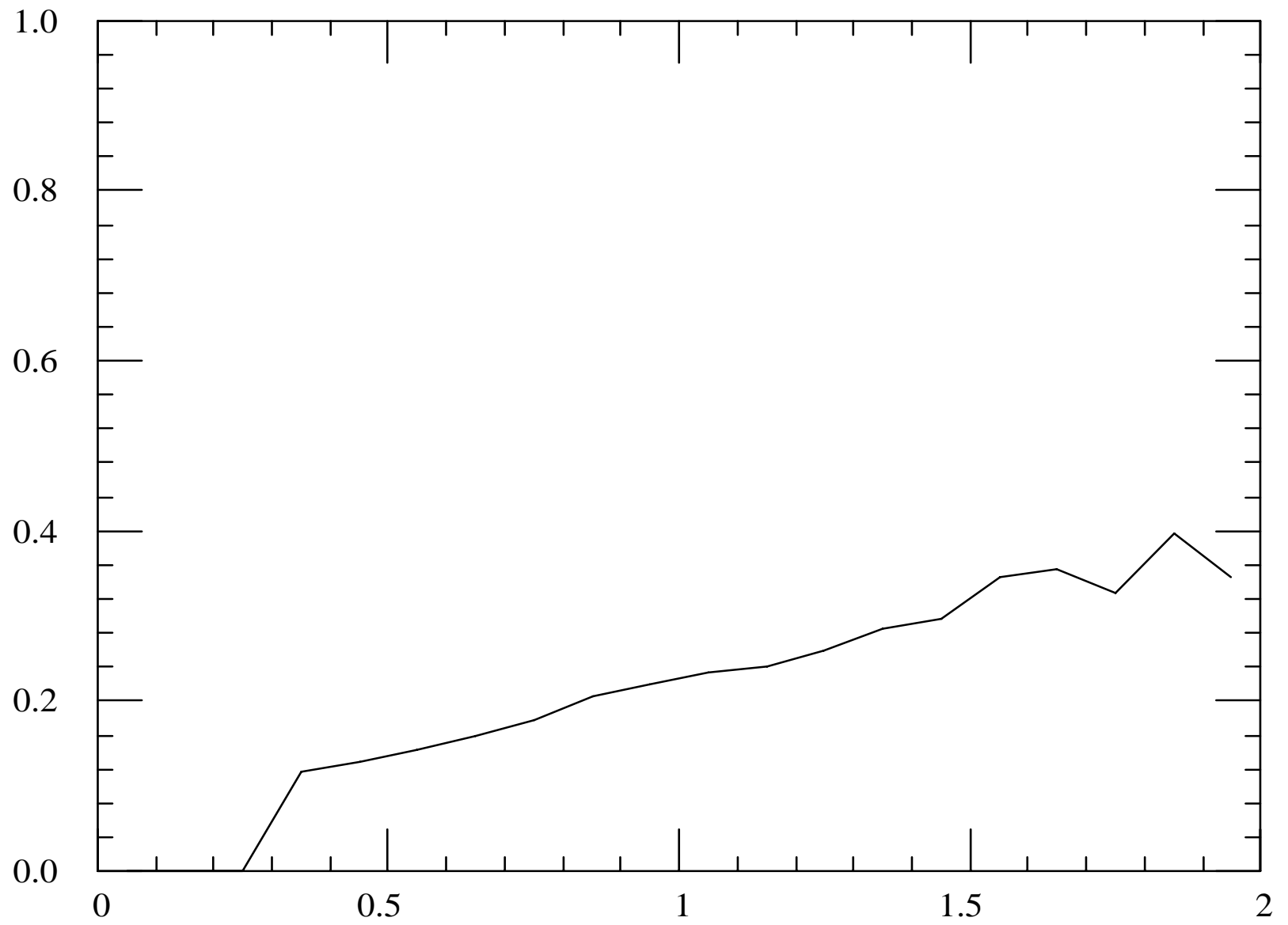
LASS only fig. 1

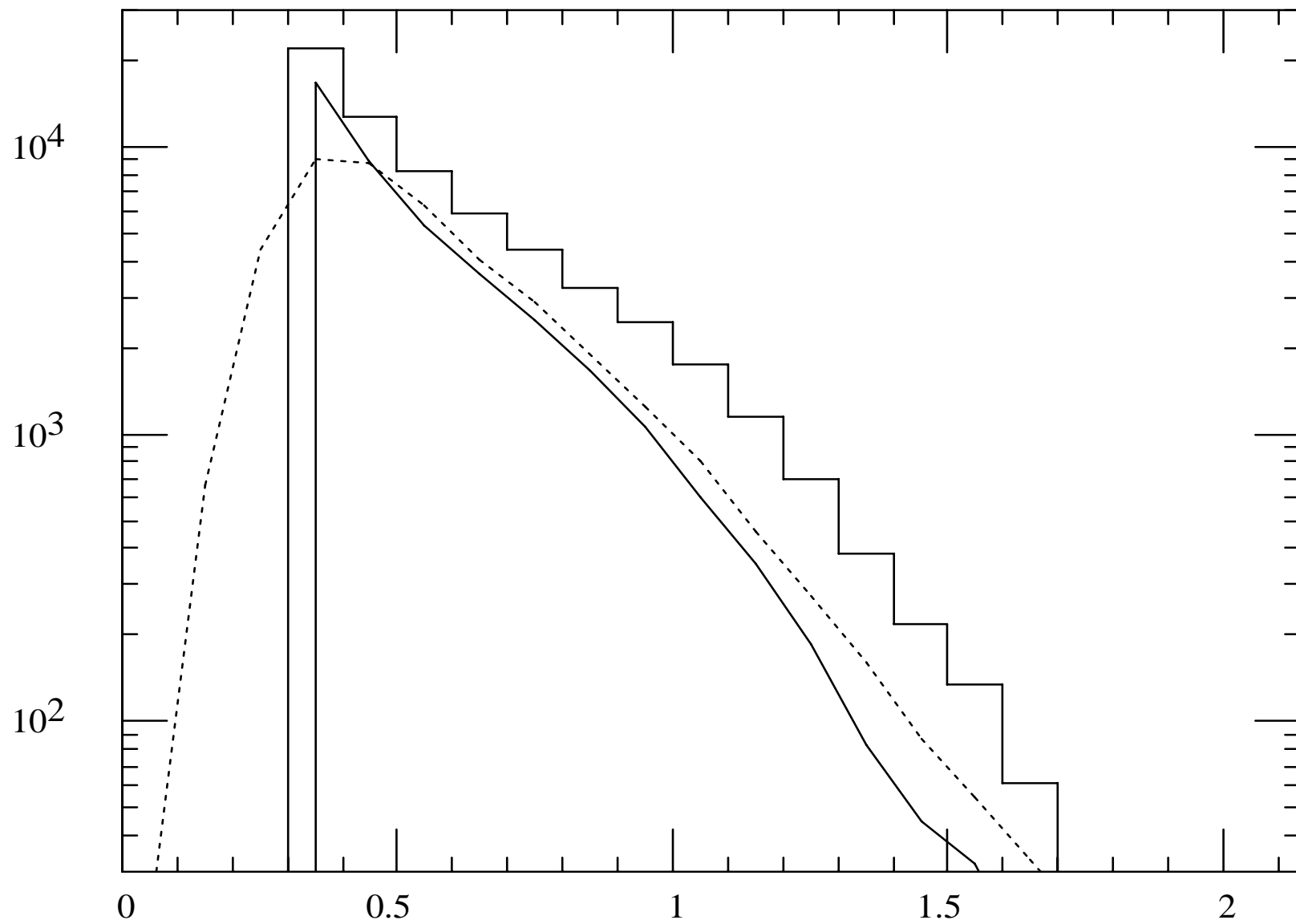


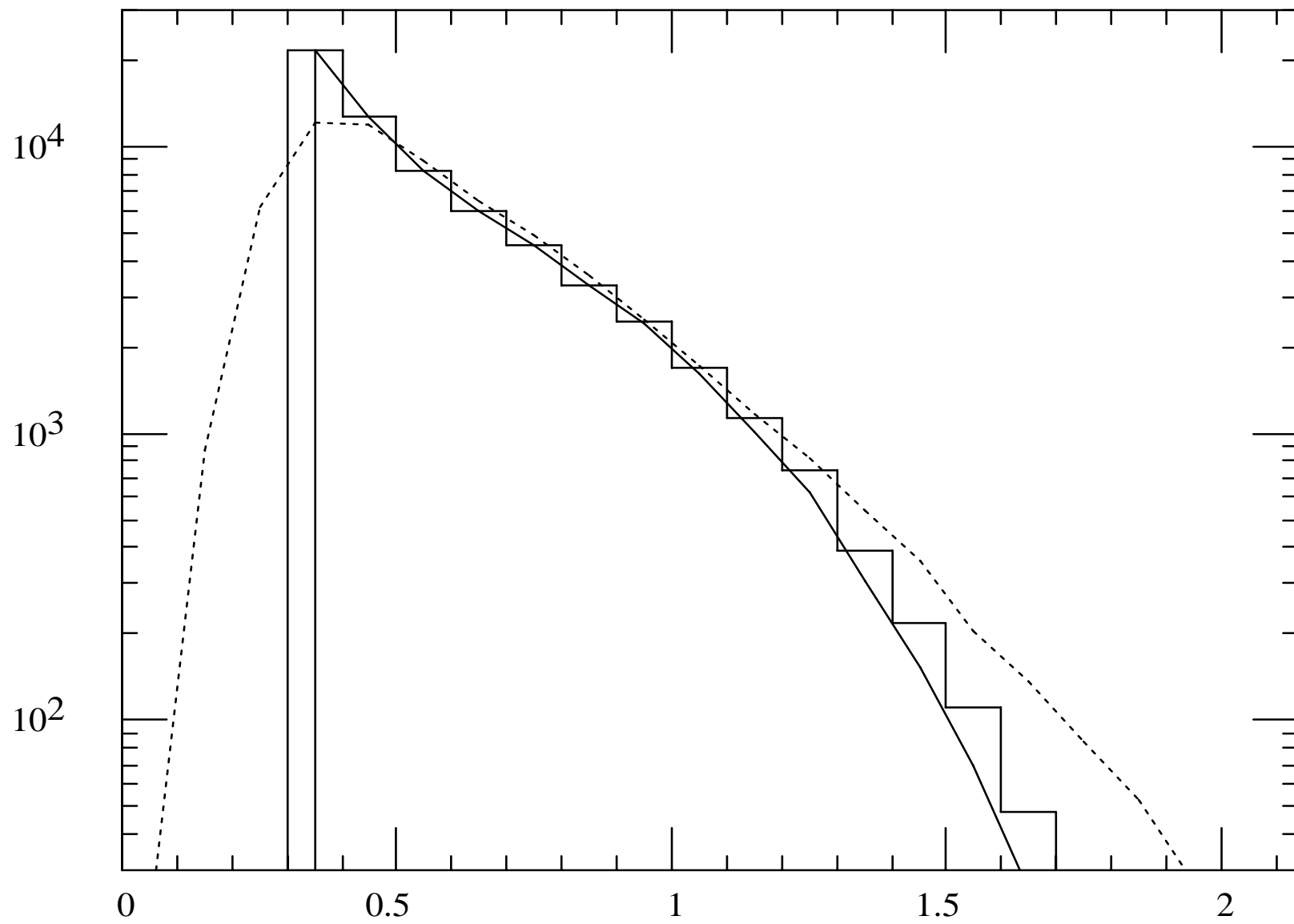
LASS only fig. 2

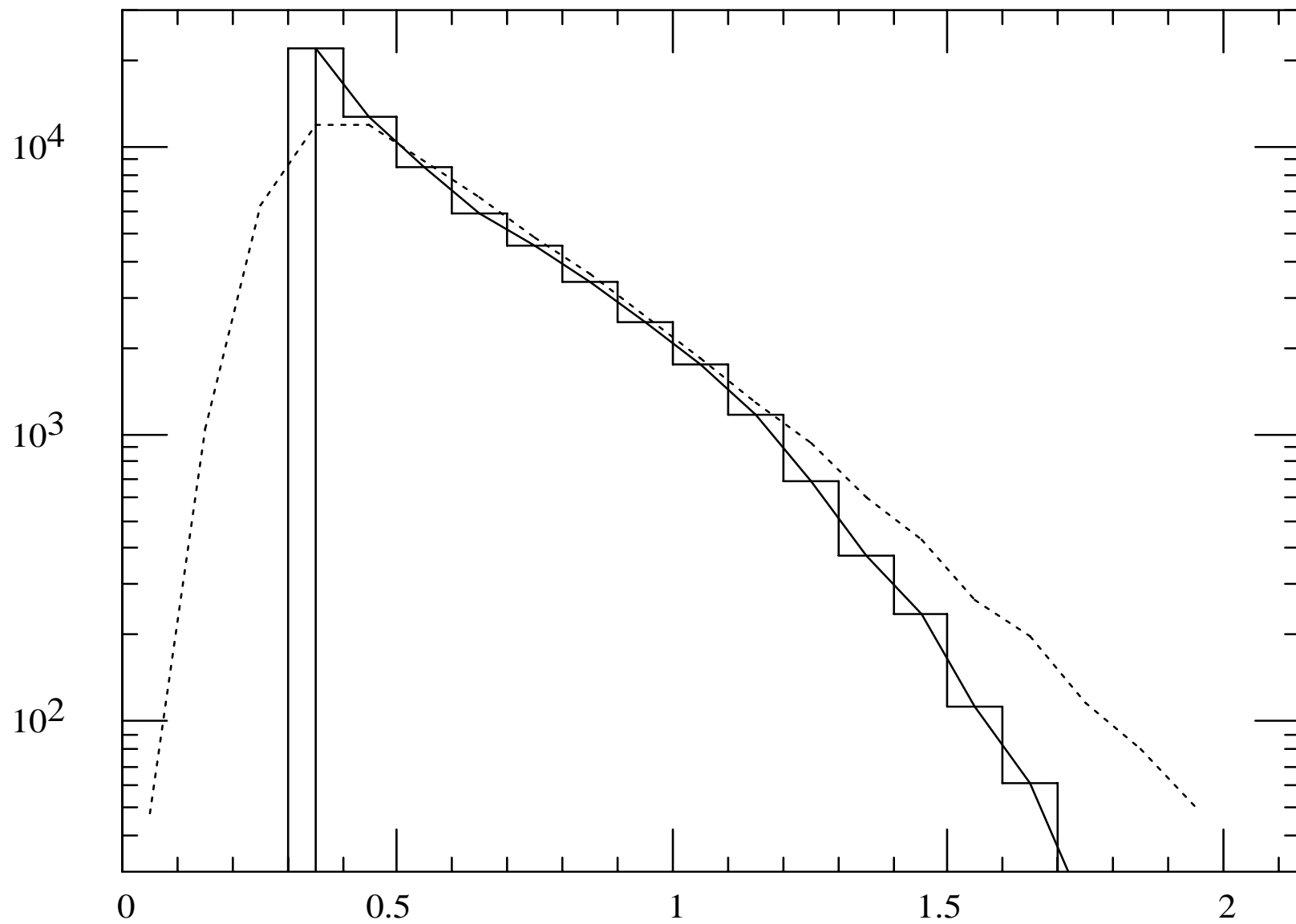


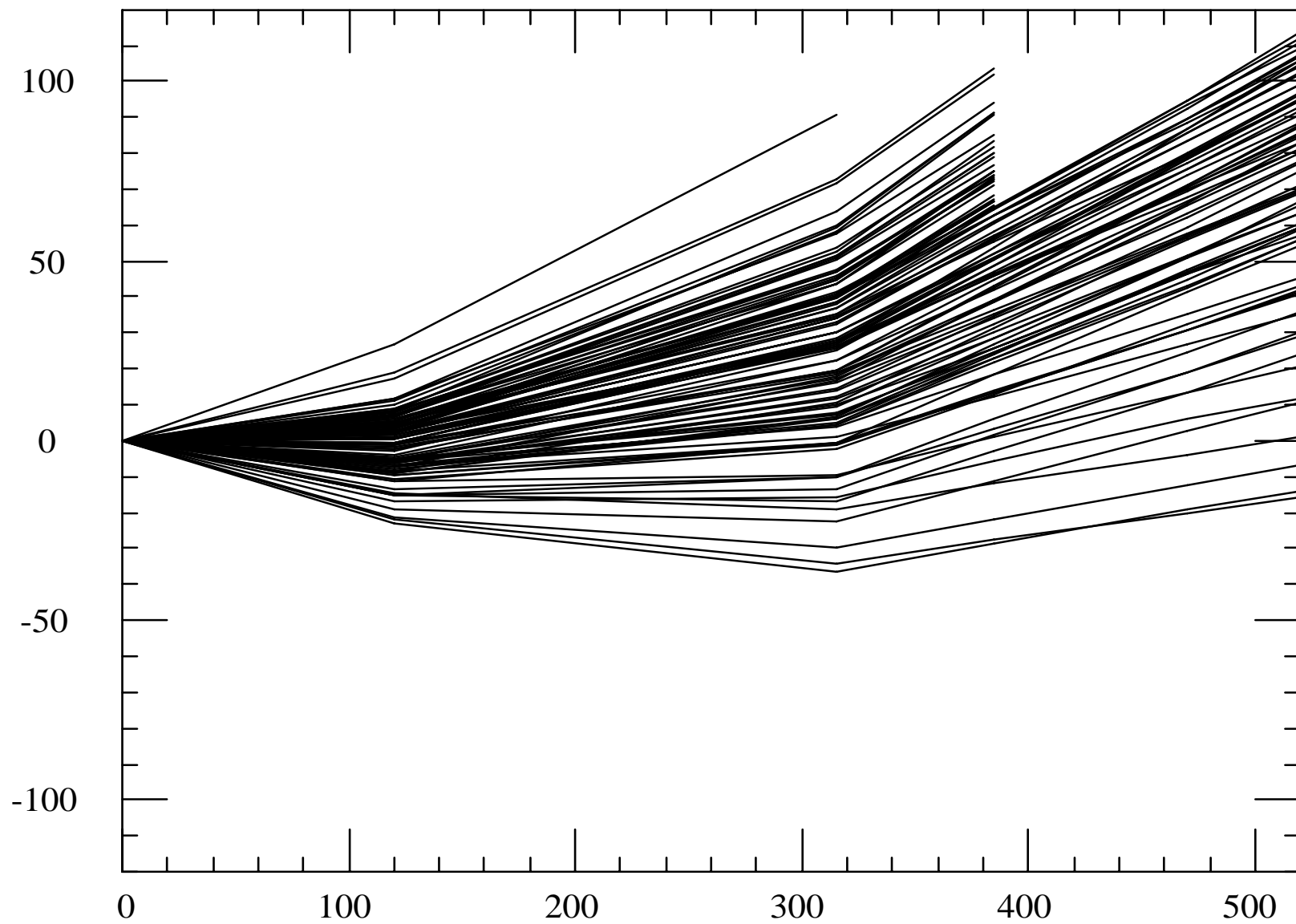
LASS only fig. 3

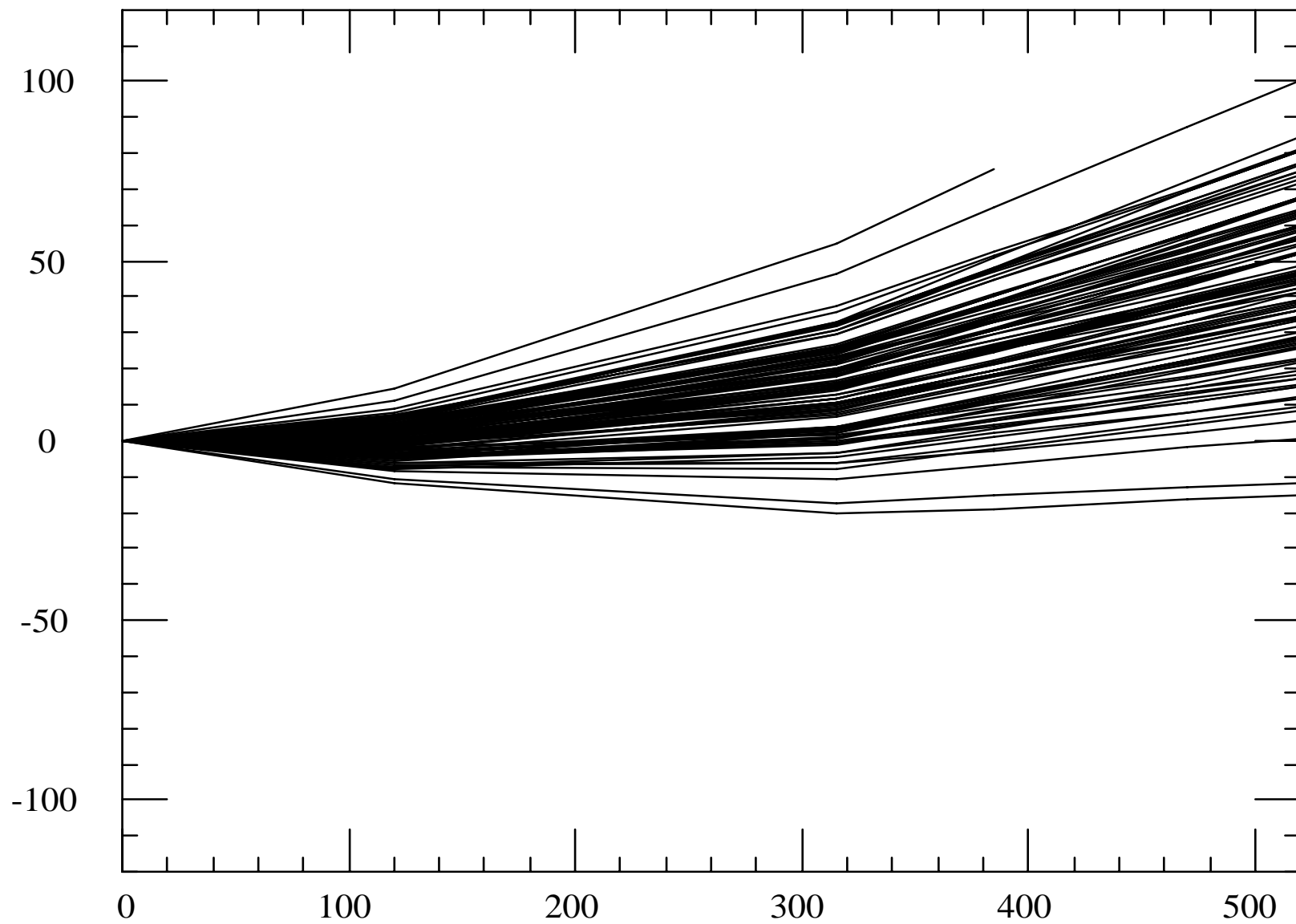


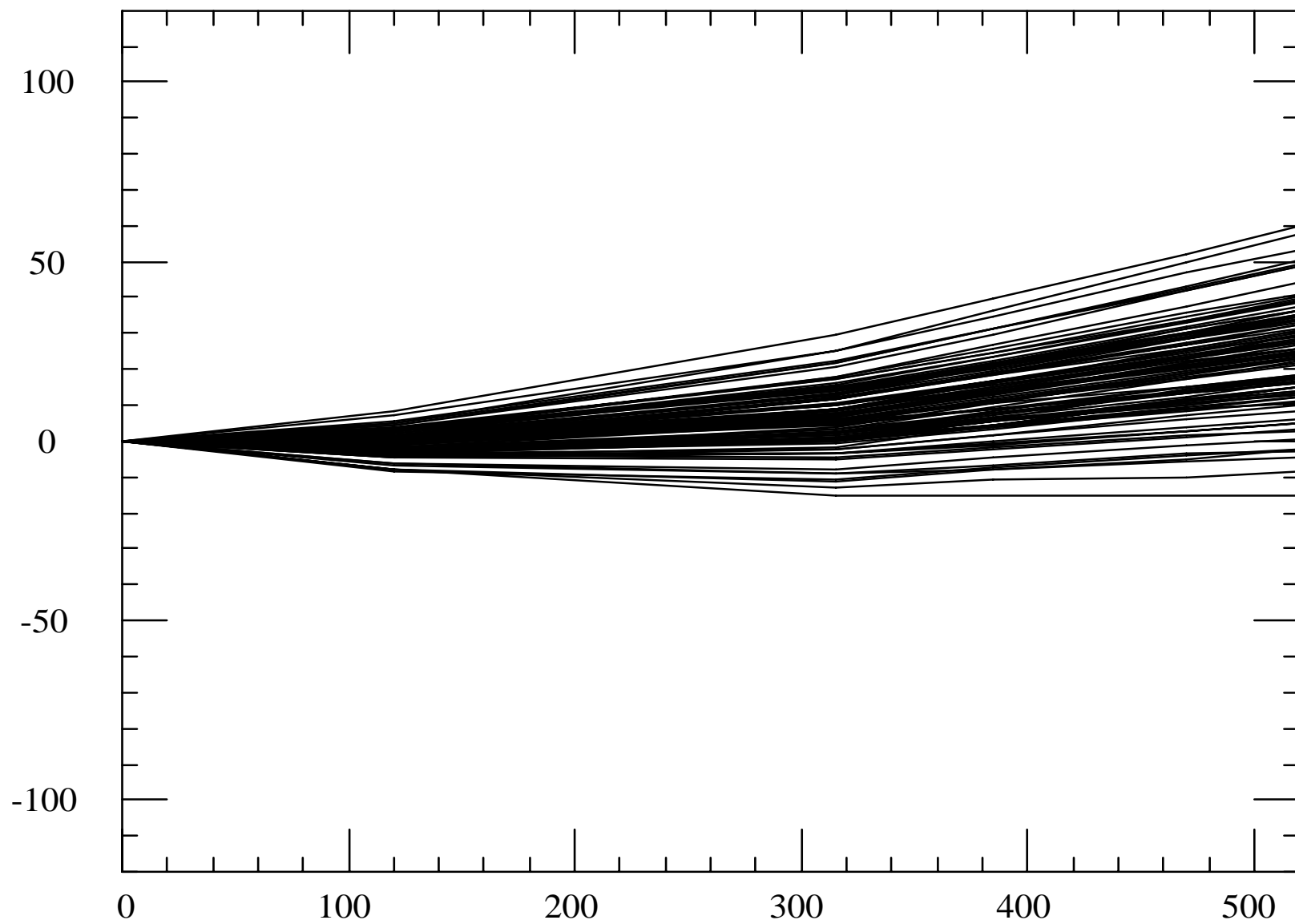




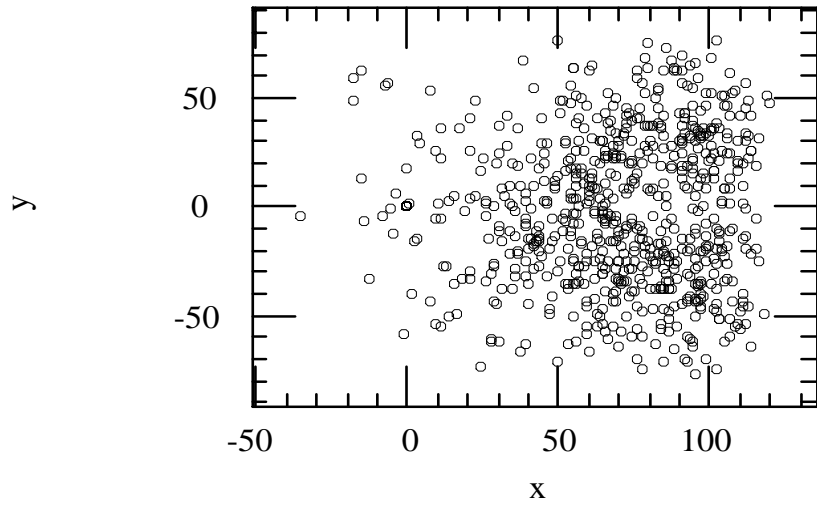




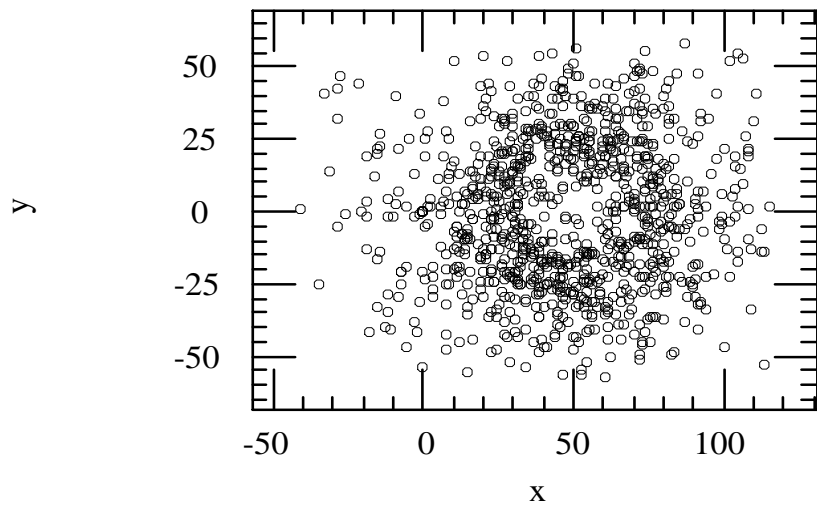




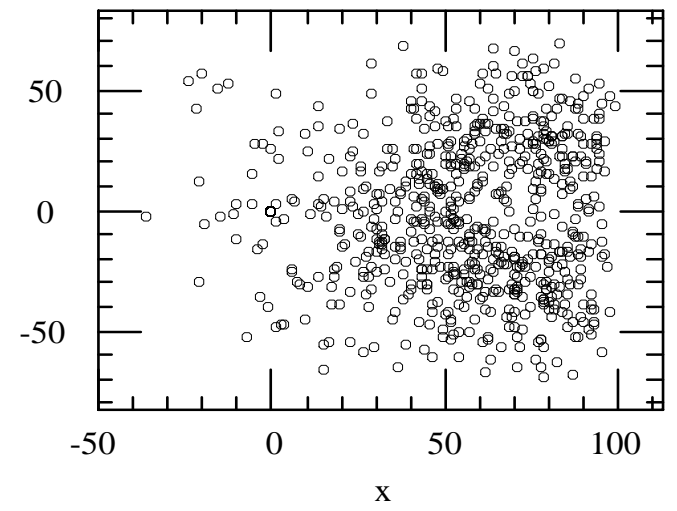
plane 5



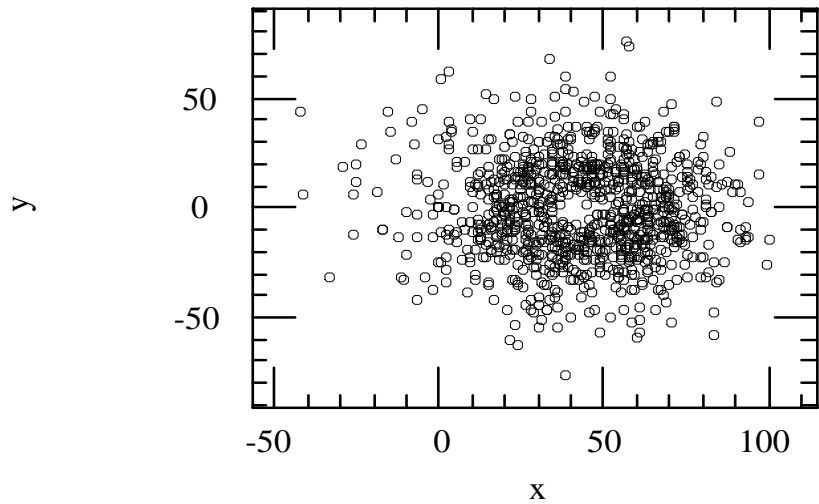
plane 3



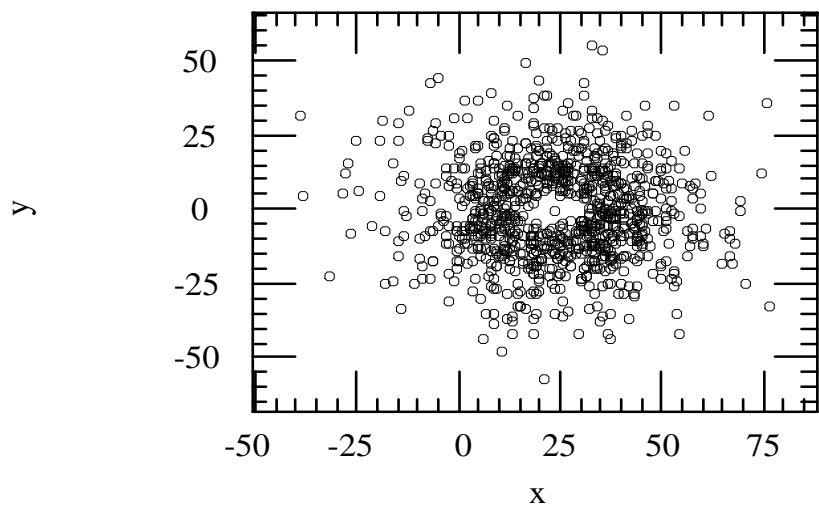
plane 4



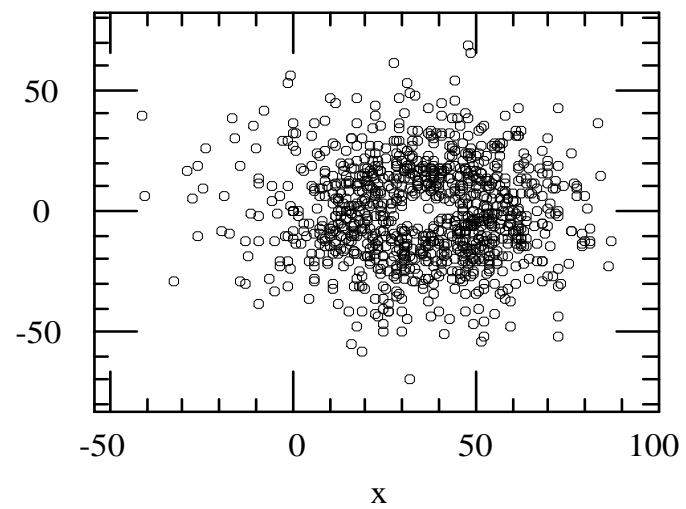
plane 5



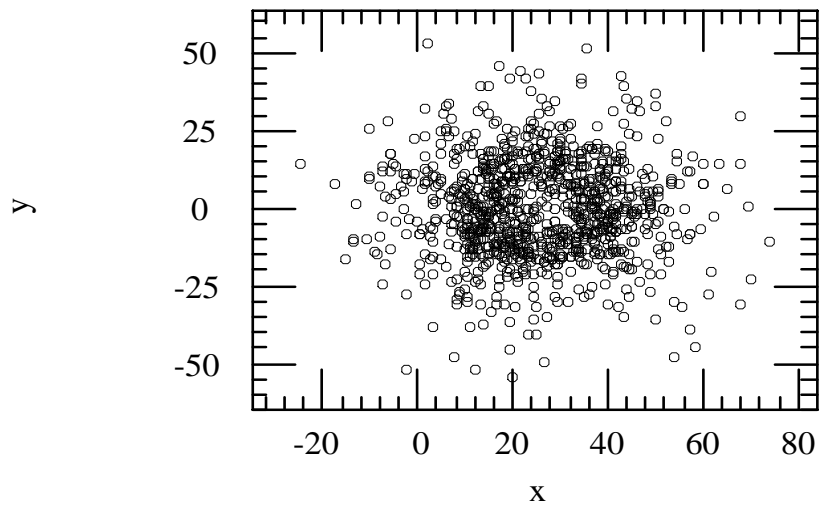
plane 3



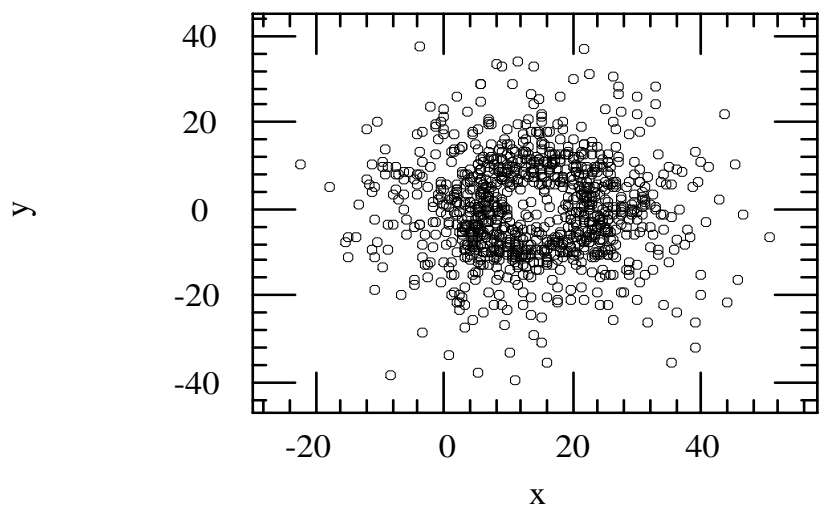
plane 4



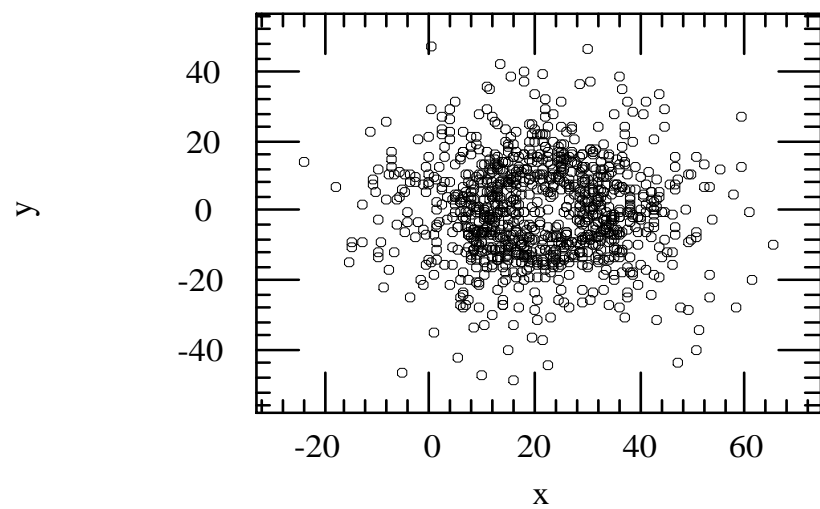
plane 5



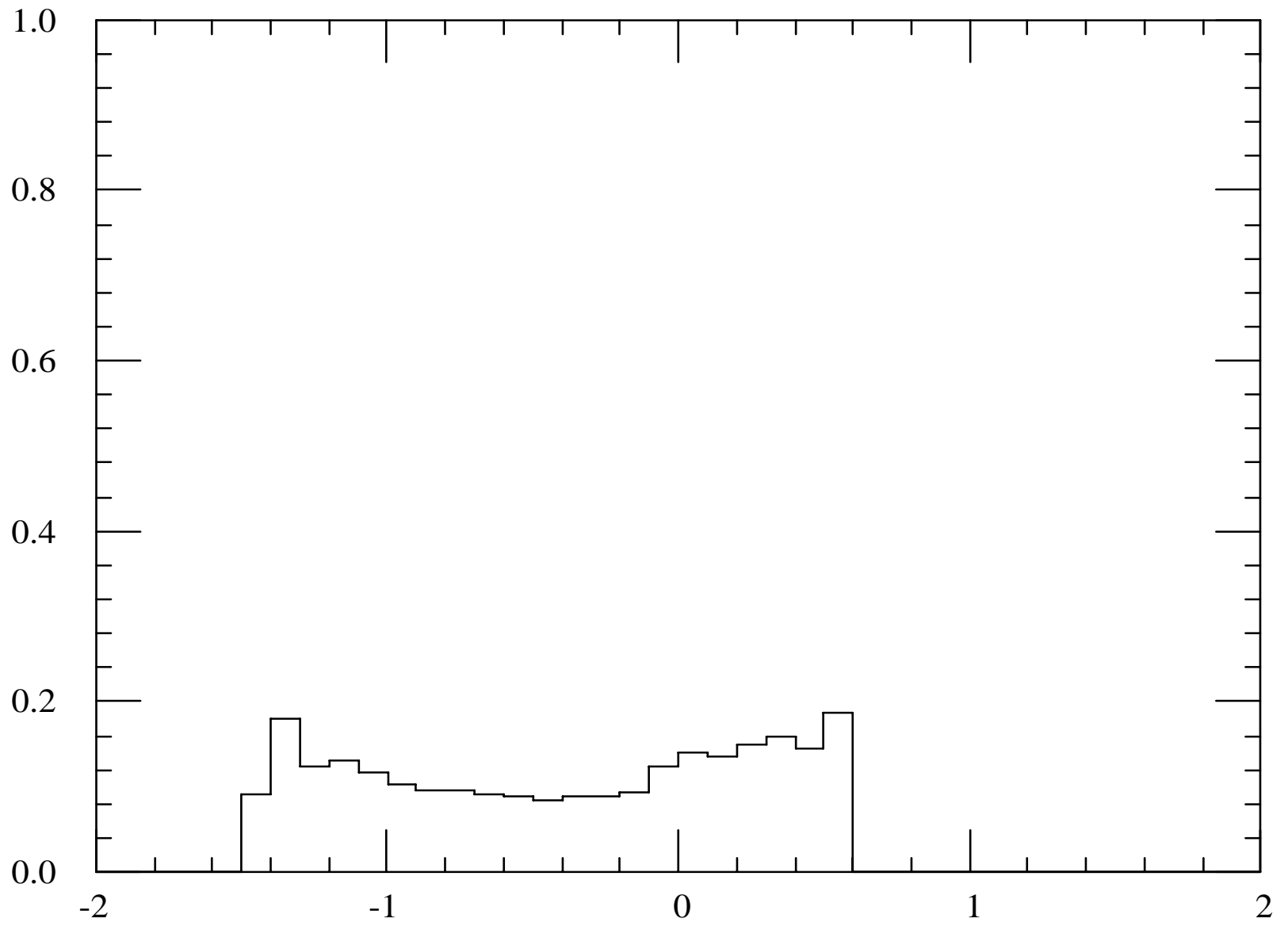
plane 3



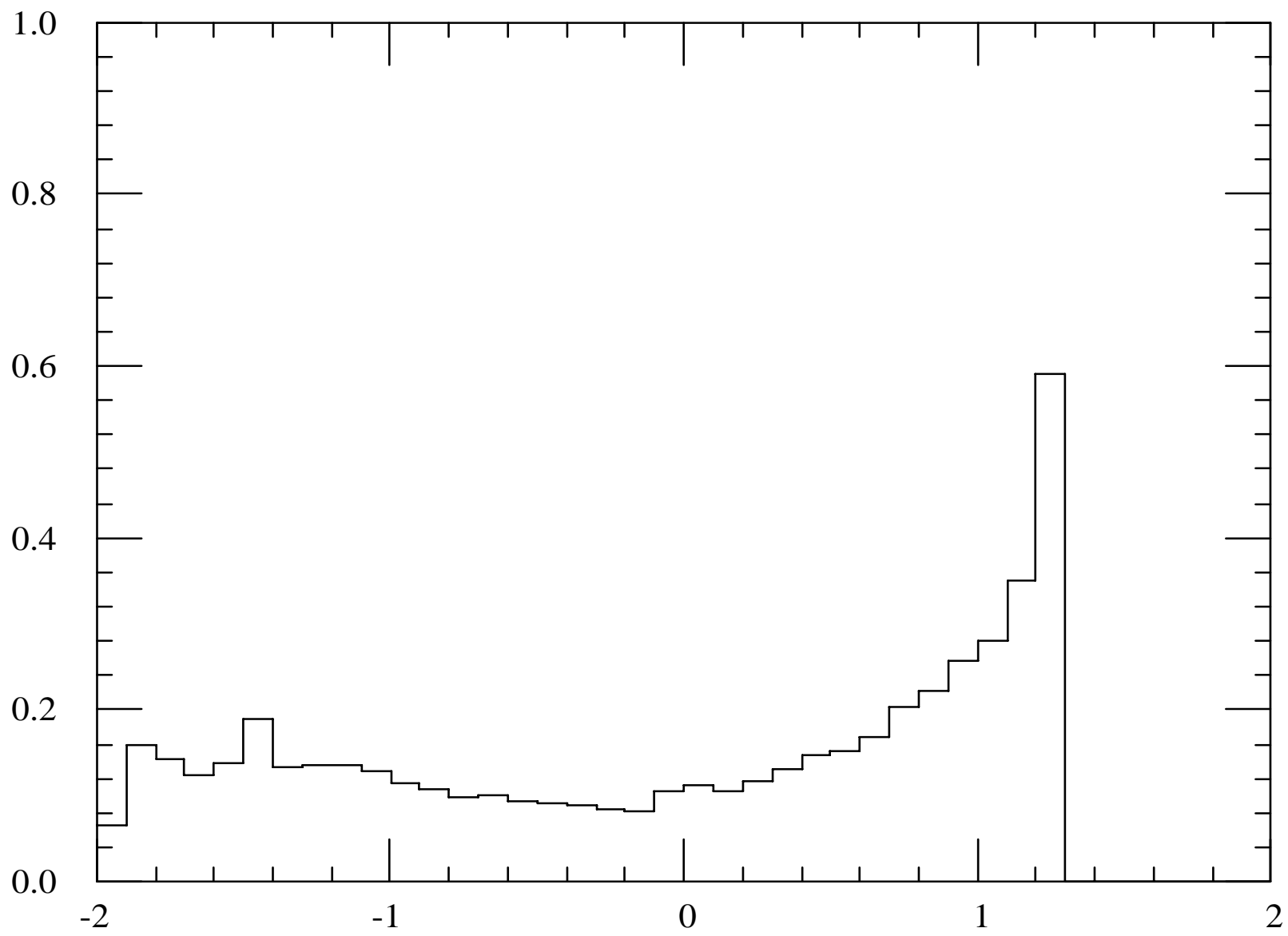
plane 4



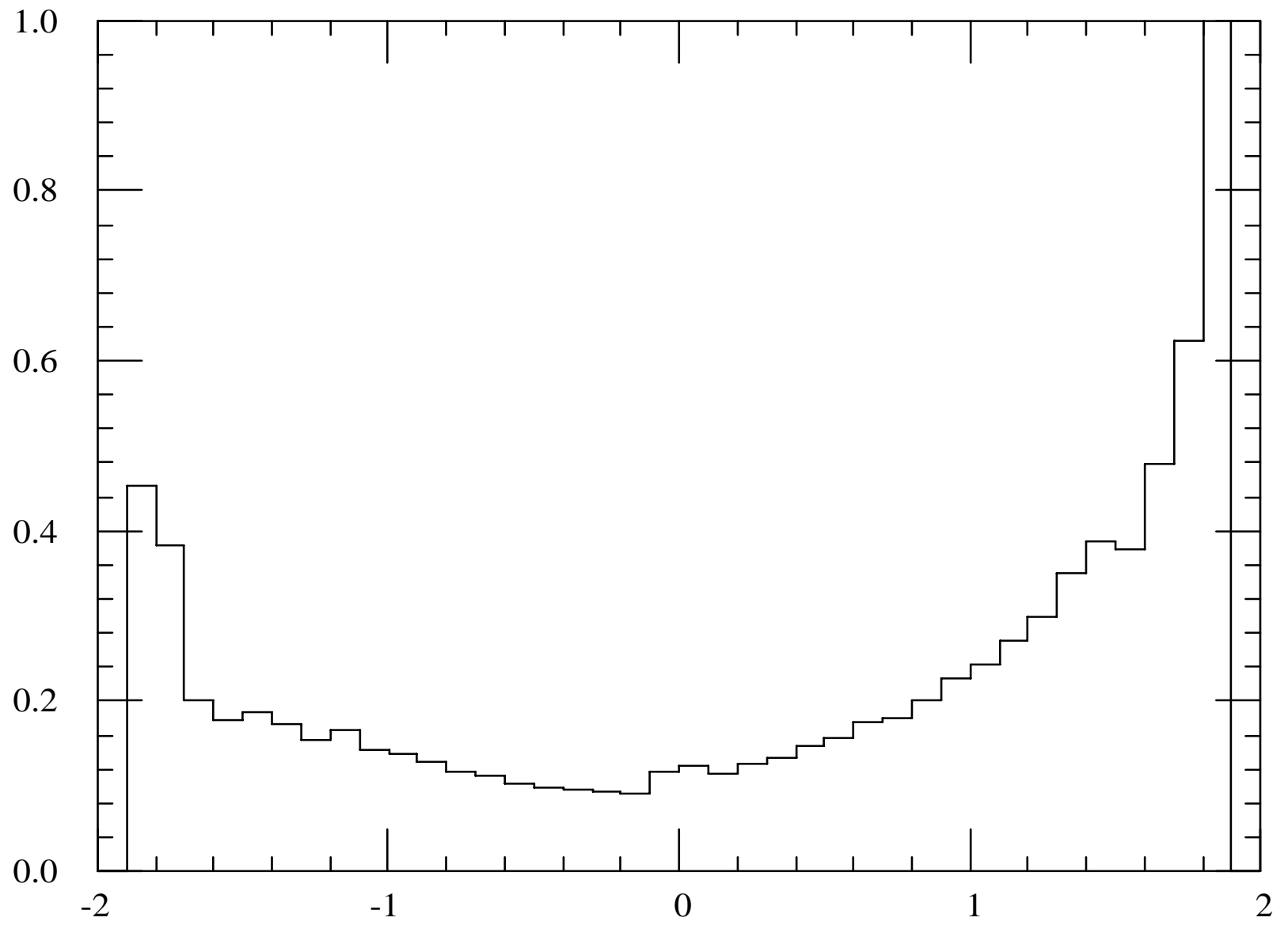
LASS real fig. 1

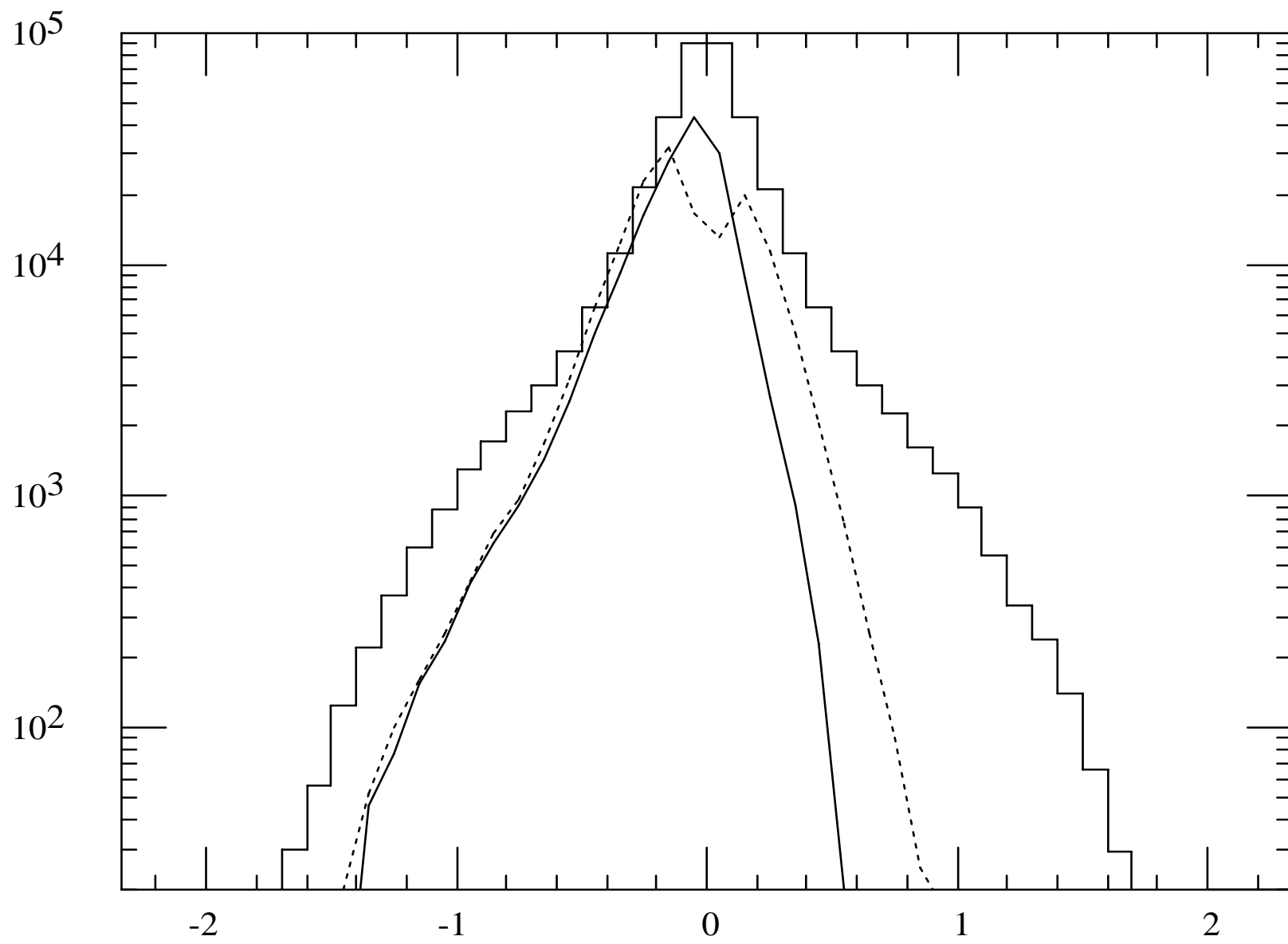


LASS real fig. 2

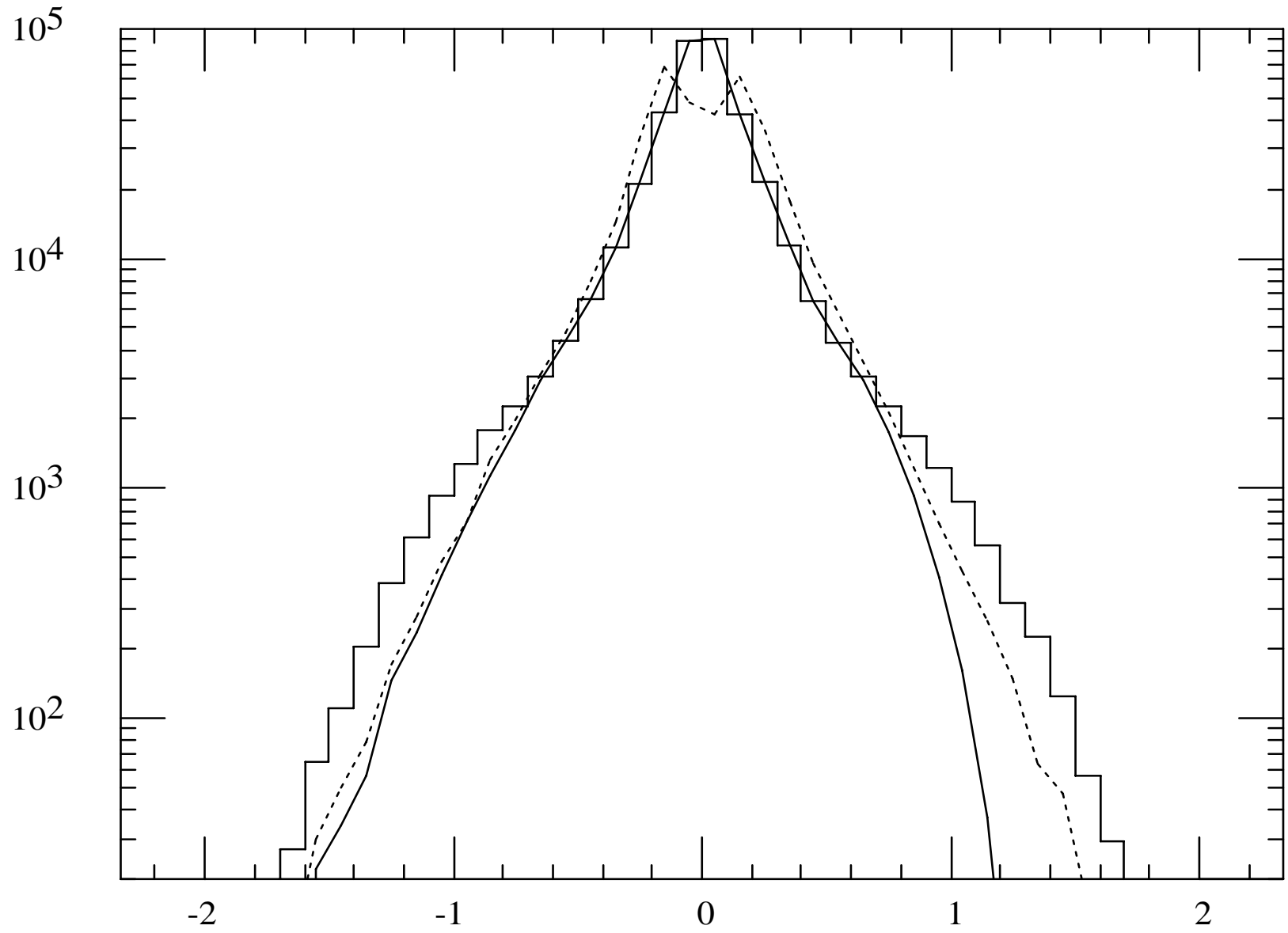


LASS real fig. 3

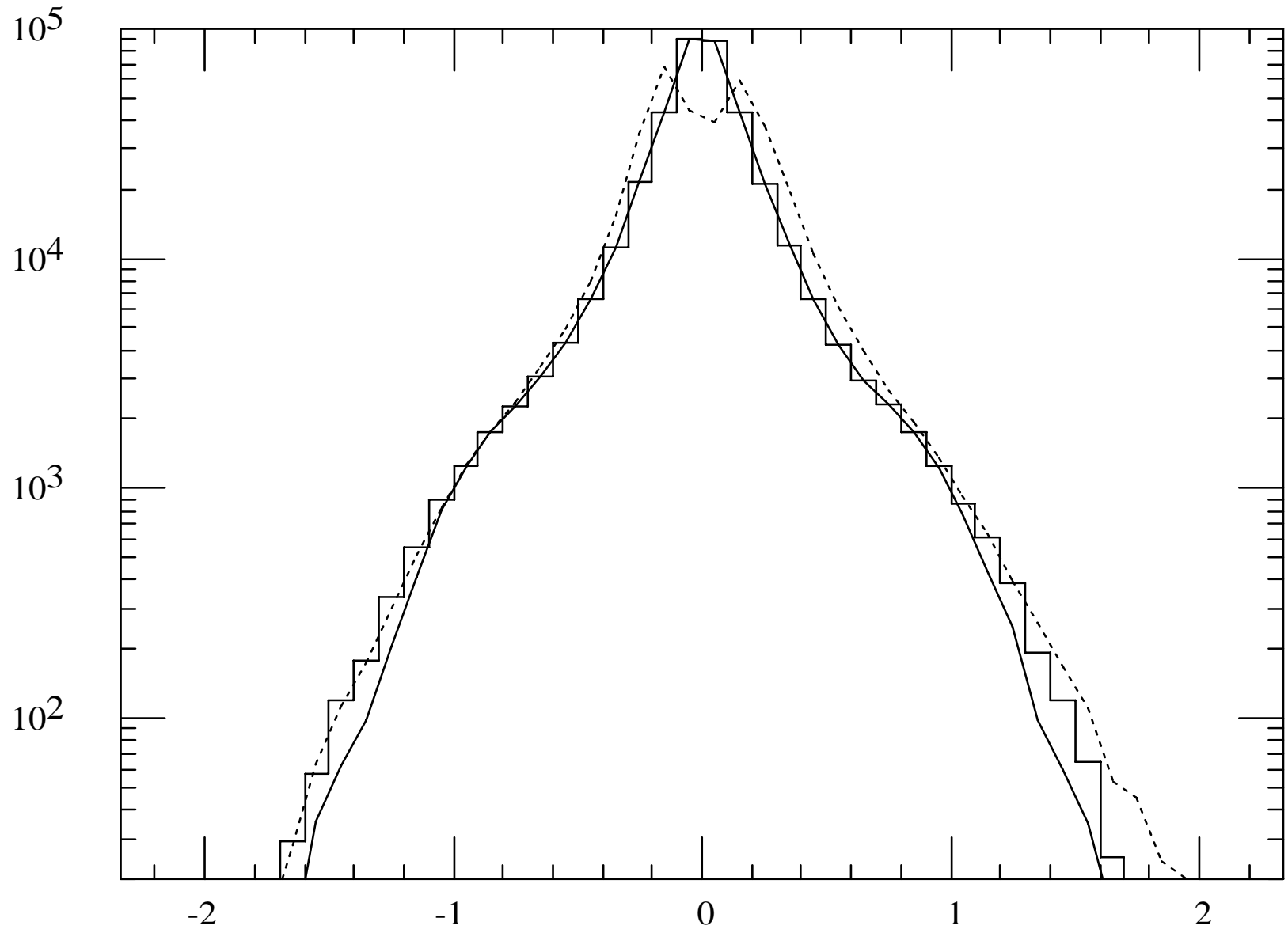




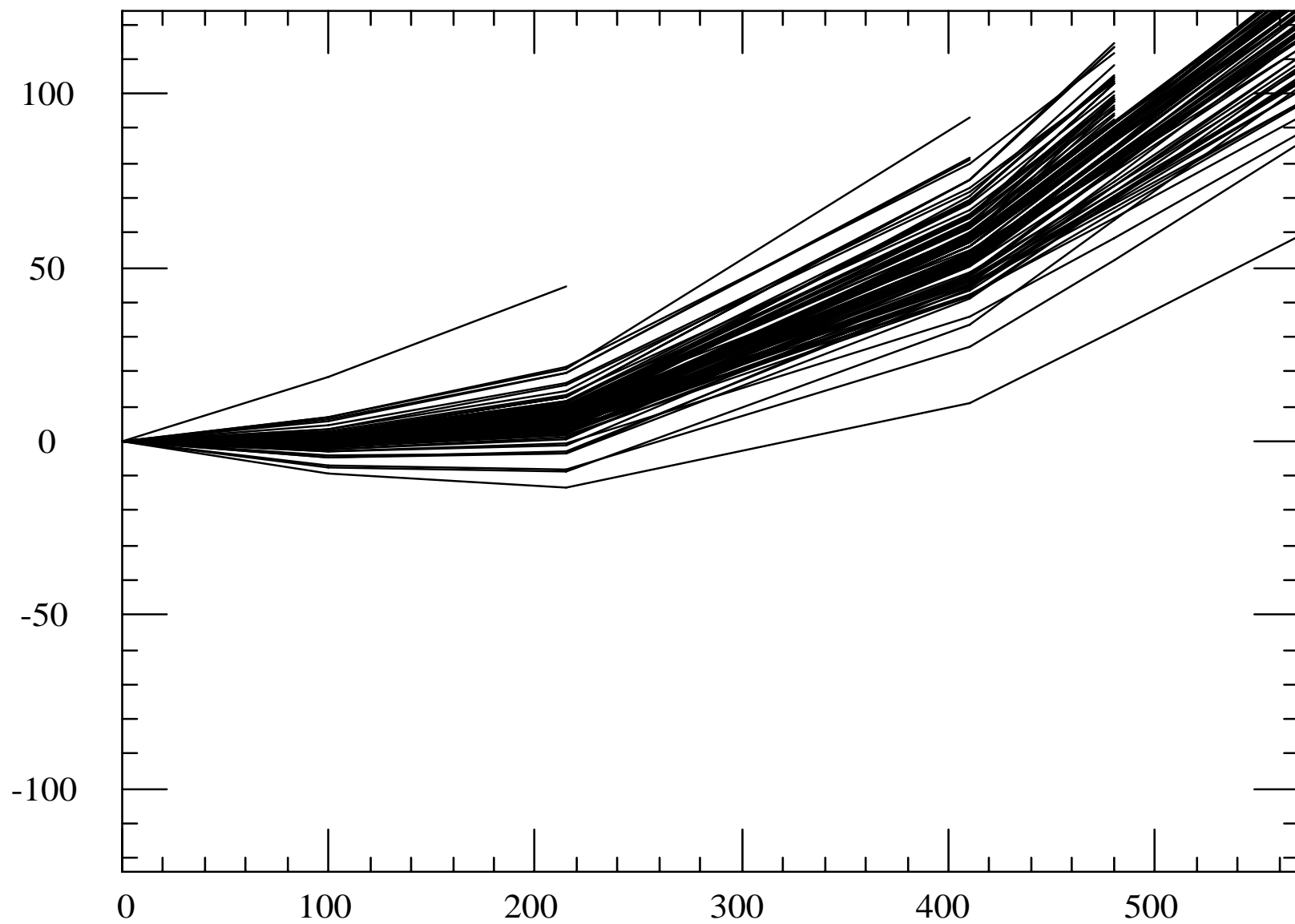
LASS real fig. 5



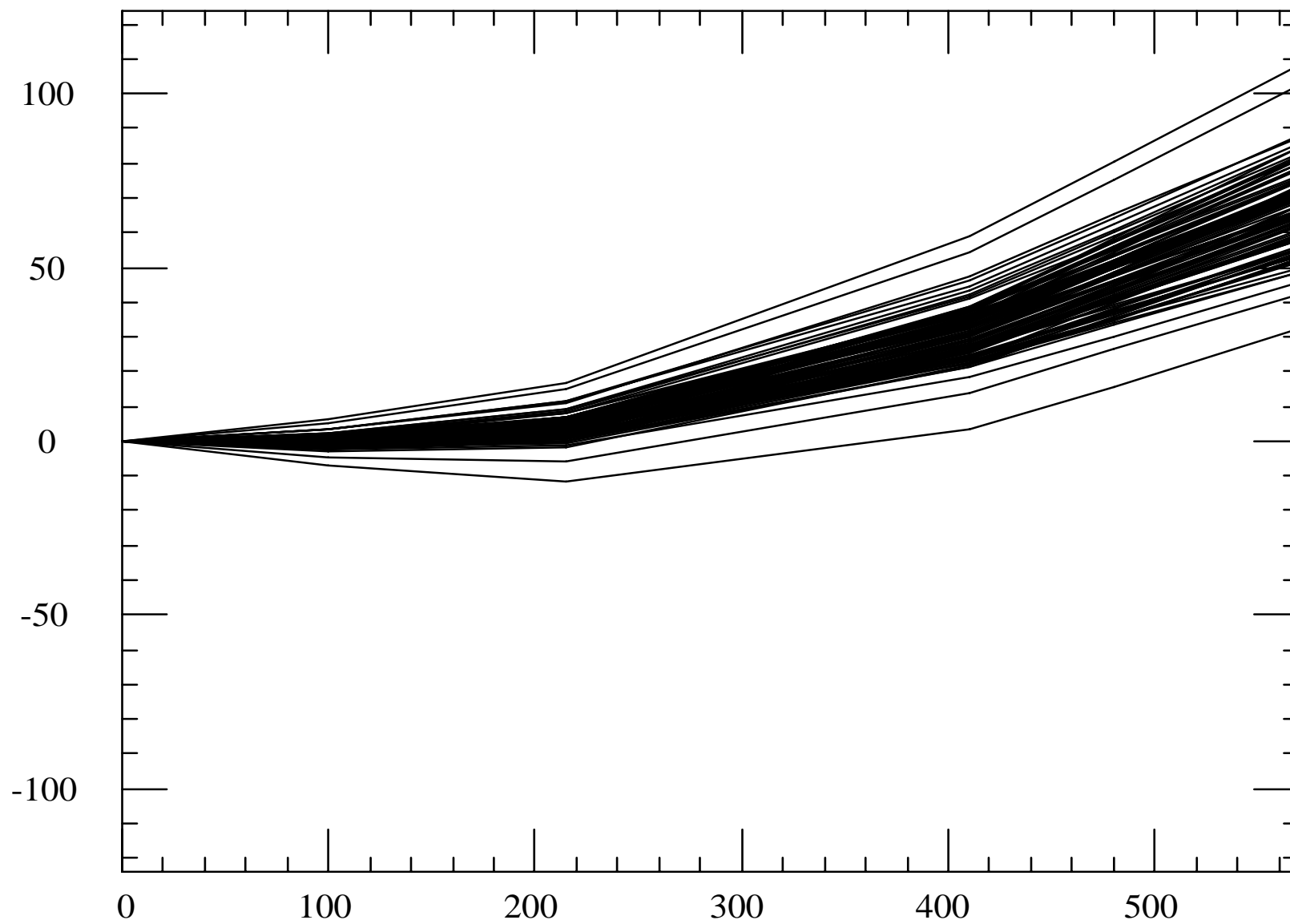
LASS real fig. 6



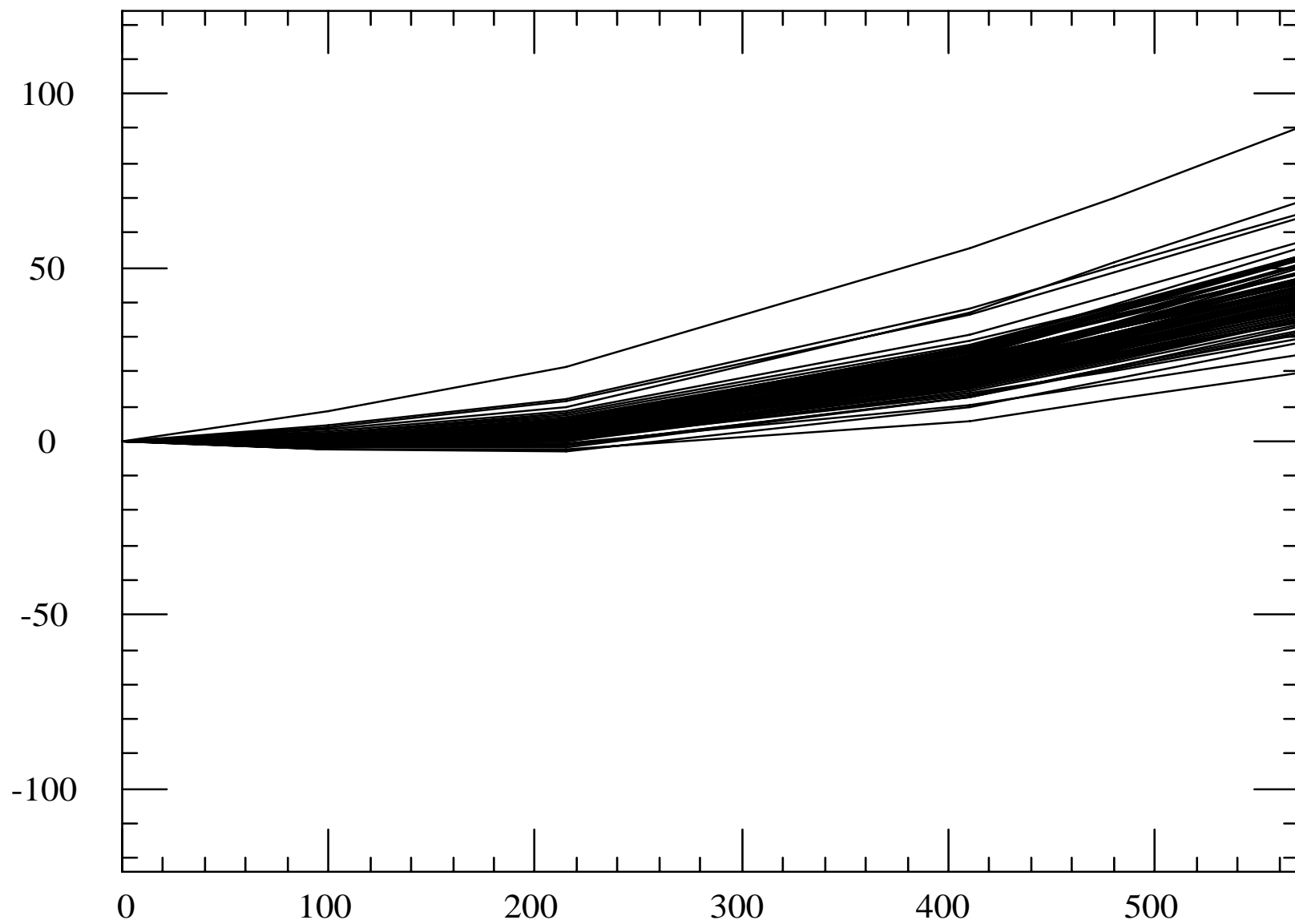
LASS real fig. 7



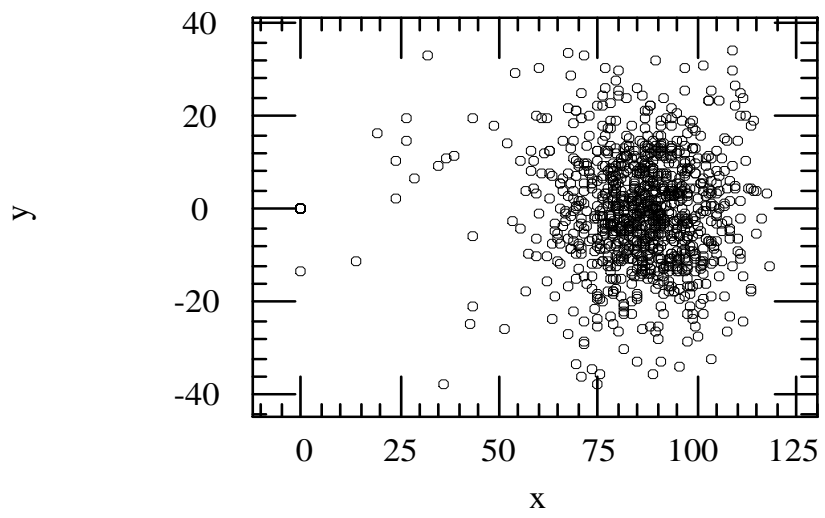
LASS real fig. 8



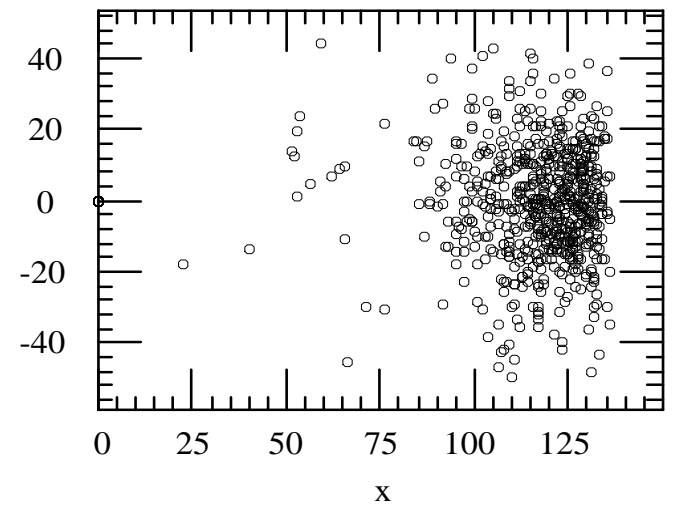
LASS real fig. 9



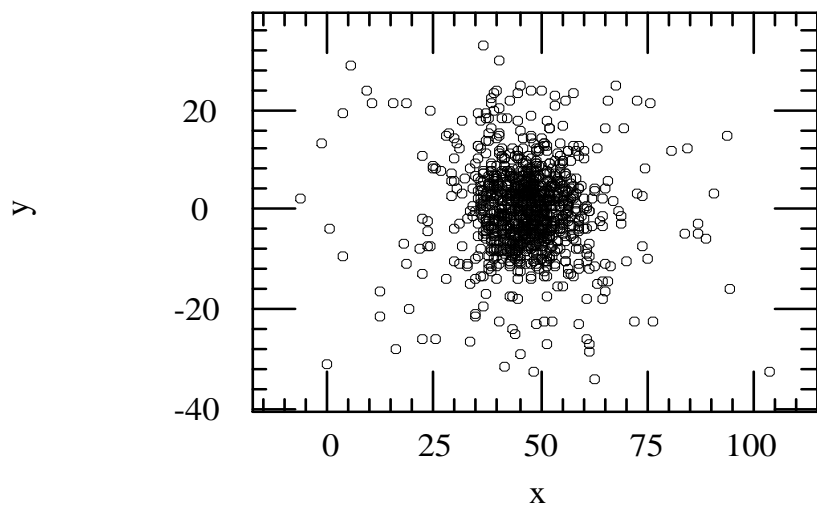
plane 4



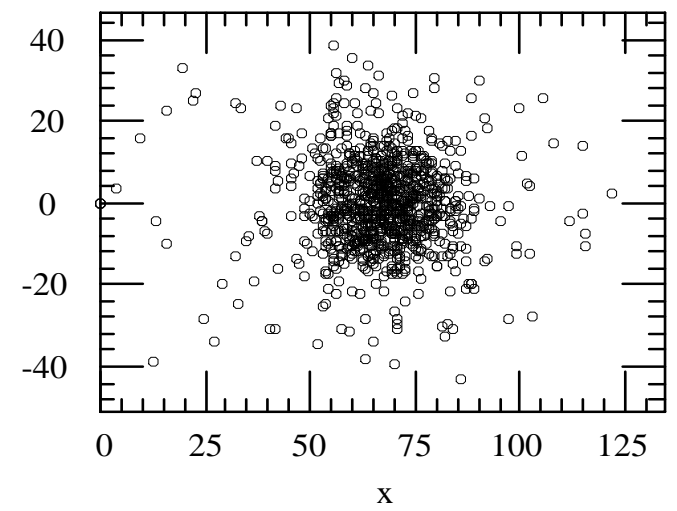
plane 5



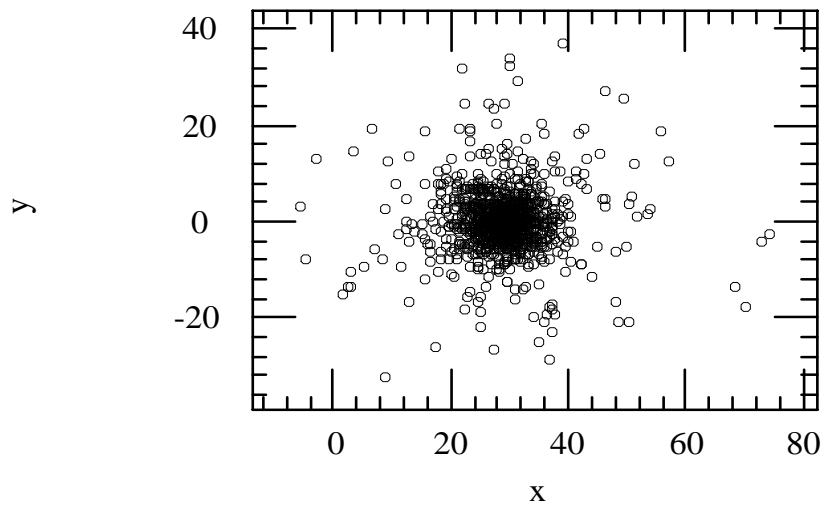
plane 4



plane 5



plane 4



plane 5

